

Advan. High Pressure Res., 2, 101-68 (1969)

IS UNDER HIGH PRESSURE

1). *C. r. hebd. Séanc. Acad. Sci., Res. 1*, 287.
42.
(1967). *Phys. Chem. Glass* **8**, 1.
d Daniels, W. B. (1966). *Phys.*

Stand. 68A, 97.
va, E. Ya. and Popova, S. V.
verd. Tela **6**, 2223).
gina, L. M. (1965). *Soviet Phys.*
326).

Research and Development Center
l Electric Research and Devel-

id. Séanc. Acad. Sci., Paris **264**,
Res. Bull. 2, 819.
es. Bull. 2, 889.

tré, M. and François, D. (1966).
1).
hemistry", 3rd Edn. Clarendon
ce, N. Y. **139**, 338.

on.
J. *Am. ceram. Soc.* **44**, 170.
). *Z. Kristallogr.* **125**, 450.
67b). *Inorg. Chem.* **6**, 1872.

s" Vol. 1, 2nd Edn. Interscience,
" Vol. 2, 2nd Edn. Interscience,
and Forrat, E. F. (1963). *Acta*

41, 827.
C. M. (1963). In "High Pressure
C. Lloyd, p. 262. Butterworths,

, 749.
Soviet Phys. Crystallogr. **12**, 28

CHAPTER 2

Some Aspects of High Pressures at Low Temperatures

J. S. DUGDALE

*Department of Physics, University of Leeds,
Leeds 2, England*

I. Introduction	101
II. Techniques	102
A. Liquid helium	103
B. The ice-bomb technique	103
C. Direct compression in piston-cylinder arrangement	103
D. Frozen oil-kerosene	104
E. Clamp techniques	104
F. Helium gas	104
III. The Fermi Surface as a Function of Pressure	107
A. Experimental	108
B. Nearly-free-electron model for Zn	115
C. The pseudo-potential method	121
D. Comparison of theory with experiment	129
IV. Effect of Pressure on Electrical Conductivity	142
A. Phonon-scattering processes	142
B. Temperature and pressure dependence of resistivity at very low temperatures	146
C. Effect of temperature and pressure on electrical resistivity at high temperatures	147
D. Change of <i>K</i> with volume	150
E. Theoretical work	156
F. Impurity scattering	162
G. Phonon and impurity scattering both present	163
V. Some Conclusions	164
References	166

I. INTRODUCTION

Three main reasons for wanting to use high pressures at low temperatures can be distinguished as follows. In the first place, the phenomenon to be studied may itself be specifically confined to low temperatures. We know from the third law of thermodynamics that a system in internal thermodynamic equilibrium must take up an "ordered" state at sufficiently low temperatures; we may regard the onset of superconductivity or magnetic transitions in certain alloys and insulators as examples of this general tendency. To study such transitions

under pressure thus demands the combination of low temperatures and high pressures.

In the second place, we may wish to work at low temperatures simply to get rid of thermal motion and its complications. As we approach the absolute zero, we reach a condition where all changes are governed by mechanical, as opposed to thermodynamic, criteria of stability (i.e., the entropy terms in the free energy become negligible). In this way, for example, a P - V measurement can reveal and reflect rather directly the interatomic forces in a solid. Or again the mechanical properties of solids may take on a special simplicity in the absence of thermally activated processes.

Thirdly, the technique of investigation may itself require low temperatures. For example, most of the standard methods of determining Fermi surfaces require that the conduction electrons involved have long mean free paths and this in turn implies the use of low temperatures to diminish scattering by phonons.

In what follows we shall be concerned mainly with the effect of pressure on electrical conductivity in metals, in particular at low temperatures. However, in order to understand these effects, we need to know as much as possible about their high-temperature behaviour. Moreover, as we shall see, we must also have as much information as possible about the Fermi surface, the velocities of the conduction electrons and so on. We shall therefore also be concerned with the recent developments in which measurements of the change in Fermi surface under pressure are being studied.

In all that follows, we shall limit the discussion to the effect of *hydrostatic* pressures.

II. TECHNIQUES

To work at low temperatures with high pressures introduces its own problems. All substances under appreciable pressure become solid at very low temperatures so that we have to contend first with the problem of producing at low temperatures as good an approximation as possible to a truly hydrostatic pressure. Various methods have been used, but recent work has shown that some of these techniques are not always satisfactory. General techniques for using high pressure at low temperatures have been reviewed recently by Swenson (1964). We

tion of low temperatures and

work at low temperatures and its complications. As we add conditions where all changes are thermodynamic, criteria of free energy become negligible). Experiment can reveal and reflect the solid. Or again the mechanical simplicity in the absence

may itself require low temperature standard methods of determining transition electrons involved have implies the use of low temperatures.

is. is. ed mainly with the effect of metals, in particular at low temperatures. To understand these effects, we must look at their high-temperature behavior. We must also have as much information as possible on the surface, the velocities of the conduction electrons, therefore also be concerned with measurements of the change in properties being studied. The discussion to the effect of

UES

high pressures introduces its own complications. As appreciable pressure become solid materials have to contend first with the surface, as good an approximation as possible. Various methods have been used. Some of these techniques are not suitable for using high pressure at low temperatures. Recently by Swenson (1964). We

therefore mention here only those that are of particular relevance to work on Fermi surfaces and electrical conductivity. (But see also Dugdale, 1965; Stewart, 1965; Levy and Olsen, 1965.)

A. LIQUID HELIUM

This is a straightforward method of producing pressure changes at low temperatures, used originally by Kamerlingh Onnes and his collaborators to study how pressure alters the superconducting transition temperature (Sizoo and Onnes, 1925; Sizoo *et al.*, 1925). The method is severely limited because helium solidifies under quite small pressures at low temperatures; at 1° K, the solidification pressure is about 25 b and at 4° K about 140 b (both pressures refer to ⁴He). The method has, however, found useful applications recently (see below) and is often valuable as a check against methods of transmitting pressure that involve a solid transmitting medium.

B. THE ICE-BOMB TECHNIQUE

This method was introduced by Lazarew and Kan (1944). It uses the pressure generated (up to about 1800 b) when water solidifies on cooling at constant volume.

C. DIRECT COMPRESSION IN PISTON-CYLINDER ARRANGEMENT

In this method as originally used at low temperatures, the pressure is transmitted by solid hydrogen, the hydrogen itself being first condensed into the working cylinder and then compressed by means of a piston. The method was first used by Hatton (1955) to measure changes in residual resistivity and superconducting transition temperature under pressure. This direct-compression method, but using solid helium as the medium, has also been used by Goree and Scott (1966) (see below). The original reason for using hydrogen rather than helium was that hydrogen, at low enough temperatures, condenses as a solid whereas helium does not, except under pressure. For this reason, hydrogen is rather easier to deal with.

Brandt and Ginzburg (1962) used a direct-compression method in which friction between the specimen and the piston and cylinder was

reduced by a layer of graphite. The method could be used to very high pressures (40 kb) and the pressure, in one version, could be changed at the low temperature being used. On the other hand, in order to secure an isotropic stress, the specimen had to undergo plastic deformation. This may be allowable in some experiments such as the effect of pressure on the superconducting transition temperature or on polycrystals; but it has to be eliminated in work on galvanomagnetic properties where the damage may produce effects many times greater than those being studied (Itskevich, 1964).

D. FROZEN OIL-KEROSENE

This method has been used by Gaidukov and Itskevich (1963) and Itskevich (1964). In it the pressure (up to 15 kb) is first generated by a piston in a cylinder at room temperature where the oil-kerosene mixture is fluid. The fluid is then slowly solidified by cooling and finally the whole cylinder and piston can be cooled to helium temperatures.

E. CLAMP TECHNIQUES

These are extensions of the very-high-pressure techniques used at room temperature. They have been much used in studies of the superconducting transition temperature and may well come into greater use as the pressure range at low temperatures is extended. Some versions suffer from the disadvantage (as do the techniques A and D above) that the apparatus must be warmed to room temperature to change the pressure. Some ultra-high-pressure techniques (up to ~500 kb) have also been used at low temperatures (see, for example, Drickamer, 1965; Stager and Drickamer, 1963).

F. HELIUM GAS

In this technique the pressure is generated in fluid helium at a temperature close to, but just above, the corresponding solidification temperature (see Fig. 1). The helium is then allowed to solidify around the specimen under study by careful cooling. This process can either be at constant volume (as used originally by Dugdale and Hulbert, 1957) or at constant pressure. This latter method was introduced by

method could be used to very one version, could be changed the other hand, in order to had to undergo plastic deformation experiments such as the effect of temperature or on polycrystalline work on galvanomagnetic effects many times greater (1964).

KEROSENE

method and Itskevich (1963) and (15 kb) is first generated by a technique where the oil-kerosene is solidified by cooling and then cooled to helium temperature.

TECHNIQUES

High-pressure techniques used at room temperature may well come into greater use as the temperature range is extended. Some of the techniques A and D described here are limited to room temperature to high-pressure techniques (up to 100 kb) at low temperatures (see, for example, Swenson, 1963).

METHODS

Generated in fluid helium at a pressure corresponding to the solidification pressure when allowed to solidify around a specimen. This process can either be done hydrostatically by Dugdale and Hulbert, or the method was introduced by

Swenson and his collaborators and is a great improvement on the constant volume technique (Hinrichs and Swenson, 1961; Schirber and Swenson, 1961, 1962). It is an improvement in several ways: first the retained pressure at the lowest temperature (after cooling the solidified helium to say 1° K) is appreciably higher than in the constant volume method where about one quarter is lost, largely because of the contraction on freezing. Secondly the fluid pressure obtained

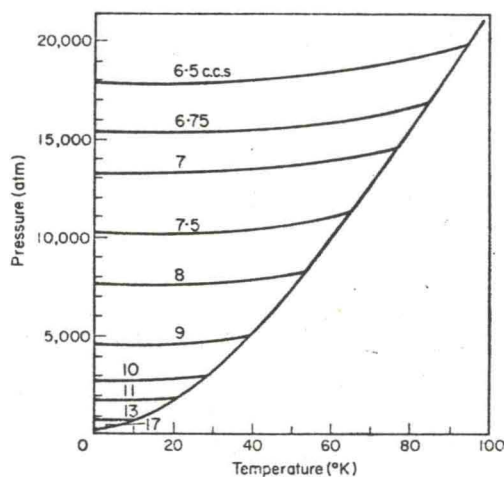


FIG. 1. Melting curve and lines of constant volume in solid ^4He : the numbers indicate molar volumes. (From Dugdale, 1958.)

is known more accurately since the correction derived from the equation of state of helium is smaller (Dugdale, 1958); see Fig. 1. And thirdly, the non-hydrostatic stresses imposed on the specimen can be made extremely small. In the solidification process at constant pressure the solid helium can grow from the fluid around the specimen from the bottom; if this is done slowly there should be no shear stresses on the specimen. Thereafter if the apparatus is cooled at constant volume, non-hydrostatic stresses will arise only because of the difference in thermal expansion or contraction of the specimen and the solid helium. At low temperatures thermal expansion or contraction is small so that there will be no appreciable relative movement of solid helium and specimen provided the initial temperature is not too high. Consequently the pressure remains essentially hydrostatic.

When we come to consider the work on Fermi surfaces we shall have occasion to compare directly the results of some of these techniques.

They show that at least at the moderate pressures at which solid helium has so far been used (below 10 kb), this method yields a very good approximation to a truly hydrostatic pressure. In addition Goree and Scott (1966) have made some direct comparisons of various methods of measuring the effect of pressure on electrical resistivity at low temperatures. They used what I have called the "helium gas" technique

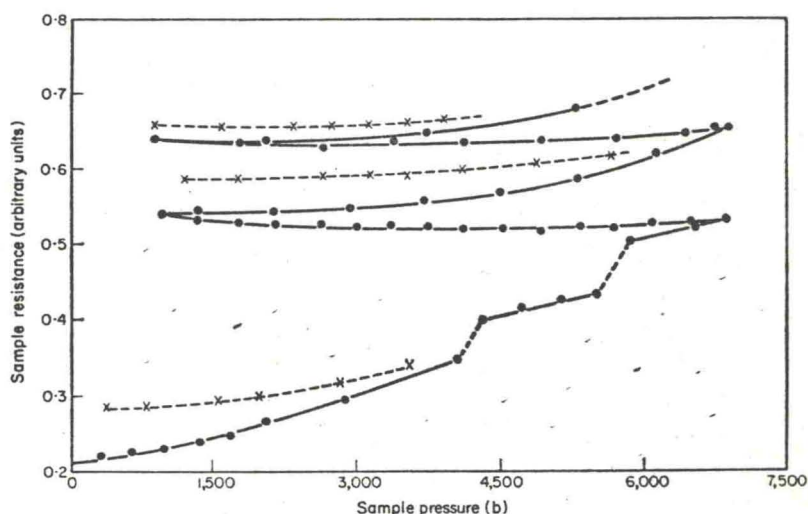


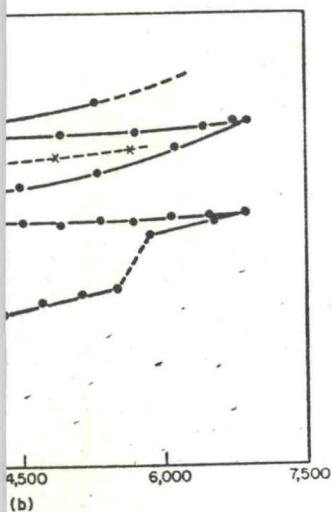
FIG. 2. Typical initial pressure cycles with Ag compressed in piston-cylinder arrangement. Sample resistance is plotted against sample pressure. (From Goree and Scott, 1966.)

(in which the solid helium is formed from the fluid at the same pressure) and the direct-compression method using both hydrogen and solid helium as the pressure medium.

Of the first, the helium gas method, they say (p. 826): "We have never encountered any case of detectable deformation or hysteresis in the resistance measurement when the experiments were carefully performed in this manner."

To test the direct-compression method, they chose a soft metal, silver, and compressed it at 4.2°K using both solid helium and solid hydrogen. They found as they expected that there was significantly less deformation of the sample (as estimated from hysteresis in its resistance values) when solid helium was used rather than hydrogen. Figure 2 shows a typical initial pressure cycle on silver obtained by the piston-cylinder method using solid helium.

te pressures at which solid
) this method yields a very
e pressure. In addition Goree
mparisons of various methods
trical resistivity at low tem-
the "helium gas" technique



(b)
Ag compressed in piston-cylinder
sample pressure. (From Goree

the fluid at the same pressure)
ng both hydrogen and solid

they say (p. 826): "We have
ple deformation or hysteresis
e experiments were carefully

l, they chose a soft metal, sil-
both solid helium and solid
d that there was significantly
imated from hysteresis in its
s used rather than hydrogen.
cycle on silver obtained by the
ium.

Although they recognized that their experiments were not comprehensive, Goree and Scott concluded: "(1) helium is a superior quasi-hydrostatic pressure transmitting medium to hydrogen in piston-cylinder apparatus, but the difference may not be great (2) Piston-cylinder experiments performed with care can give results in fair agreement with accurate hydrostatic gas experiments but they are tricky and unreliable (3) The two ice-bomb measurements [due to Kan and Lazarew (1958)] are in marked and quite unreasonable disagreement with all the others (4) The helium gas system gives consistent, reproducible results and is greatly to be preferred over the other pressure systems considered."

As we shall see below, there is other evidence to show that the ice-bomb and related techniques do not give rise to hydrostatic pressures. Goree and Scott also comment on the use of the sharpness of superconducting transitions as a criterion for having a good hydrostatic pressure. Because the ice-bomb technique could give such a sharp superconducting transition, this has been taken as evidence that the pressure was hydrostatic. Clearly this does not follow; a uniform (but non-hydrostatic) stress (e.g., a uniform shear) would give rise to a sharp transition. But even this may not be a necessary condition; it is, however, a reasonable assumption.

We now turn to the application of these methods to the determination of the properties of the Fermi surface in metals under pressure.

III. THE FERMI SURFACE AS A FUNCTION OF PRESSURE

There have been several attempts to determine how the shape of the Fermi surface of a metal changes with pressure. Here we are primarily interested in the monovalent metals, since these are in some ways the simplest theoretically, particularly from the point of view of transport properties, and since their properties have been studied more intensively than those of other metals. On the other hand metals such as Zn, Pb and Al (on which pressure measurements have recently been made), have been shown to approximate well to the nearly free electron model of a metal. For this reason and because the work on Zn makes possible a direct comparison of several high pressure techniques we shall begin by having a look at some of the work on the Fermi surface of these metals. In order to understand the results and the significance

of this work, we are ultimately led to consider the pseudo-potential approach to the description of the Fermi surface and to consider how it can predict pressure effects.

A. EXPERIMENTAL

The methods that have been used to determine the effect of pressure on the Fermi surface and related properties of Zn are summarized in Table I which refers to the techniques of producing the high pressures

TABLE I. Investigations of the effect of pressure on the Fermi surface of Zn

Authors	Method of investigating Fermi surface	Methods of producing pressure
Dmitrenko <i>et al.</i> (1959)	Torque de Haas-van Alphen	Ice-bomb technique
Verkin & Dmitrenko (1959)	Torque de Haas-van Alphen	Ice-bomb technique
Gaidukov & Itskevich (1963)	Magnetoresistance oscillations	Frozen oil-kerosene
Balain <i>et al.</i> (1960)	Ettinghausen-Nernst effect	Liquid helium
Schirber (1965)	Oscillations in transverse magnetoresistance	Helium gas
Higgins & Marcus (1966)	Torque de Haas-van Alphen	Alloying
O'Sullivan & Schirber (1966)	de Haas-van Alphen (modulation technique)	Helium gas Liquid helium
Melz (1966a)	de Haas-van Alphen (modulation technique)	Helium gas

already described. The methods of investigating the Fermi surface which are of importance here will now be summarized.

1. *The de Haas-van Alphen Effect (see, e.g., Shoenberg, 1957)*

This is probably the most important method of determining the shapes of Fermi surfaces. The effect discovered by de Haas and van Alphen refers to the oscillatory variation of the magnetic-susceptibility of a single crystal of a metal when the applied magnetic field, H , varies. The susceptibility is periodic in $1/H$ (more correctly $1/B$)

consider the pseudo-potential surface and to consider how

and from this period, P , the extremal cross-sectional area, A (or areas) of the Fermi surface which is normal to the field, can be determined from the relationship:

$$A = \frac{2\pi e}{\hbar P} \tag{1}$$

AL

termine the effect of pressure ties of Zn are summarized in producing the high pressures

where e and \hbar have their usual significance.

From the temperature dependence of the *amplitude* of the effect, the effective mass

$$m_c^* = \left(\frac{\hbar^2}{2\pi} \right) \frac{\partial A}{\partial E} \tag{2}$$

of pressure on the Fermi

for the relevant extremal orbit can be found. Once this is known, the life time, τ , of the electrons in that orbit can also be found from the *field* dependence of the amplitude.

	Methods of producing pressure
	Ice-bomb technique
	Ice-bomb technique
	Frozen oil-kerosene
	Liquid helium
verse	Helium gas
	Alloying
	Helium gas
que)	Liquid helium
n	Helium gas
que)	

In order to observe the effect $\omega_c \tau$ should be comparable or large compared to unity and $\hbar \omega_c \gg kT$. Here ω_c is the appropriate cyclotron frequency; $\omega_c \equiv \frac{eB}{m_c^*}$. The first condition on ω_c implies that high fields are needed and long relaxation times, i.e., very pure materials at low temperatures so that the conduction electrons are not scattered too frequently by either impurities, imperfections or phonons. The second condition ensures that separation of the Landau levels is large compared to their thermal broadening.

There are several techniques commonly in use for observing de Haas-van Alphen oscillations.

estigating the Fermi surface e summarized.

e.g., Shoenberg, 1957)

1. *The torque method.* In this the specimen is suspended from a torsion element in a uniform magnetic field. The couple on the element is then measured as a function of magnetic field for different relative orientations of crystal and field. The method is generally used for looking at small parts of the Fermi surface with comparatively small cross-sections.

method of determining the discovered by de Haas and tion of the magnetic-suscepti- on the applied magnetic field, e in $1/H$ (more correctly $1/B$)

2. *The pulsed-field method.* In this technique large magnetic fields (up to, say, 200 kG) are produced by discharging a bank of condensers through a coil in which the specimen (suitably cooled) is placed. The magnetization of the specimen is measured by a pick-up coil surrounding the specimen; effects due to the changing magnetic field are largely compensated by means of a second pick-up coil connected in opposition

to the first and subject to the same field. The output from the pick-up coils is then displayed on a cathode-ray tube, along with a signal representing the field variation. This display can then be photographed and the period of the oscillation can subsequently be measured.

3. *The modulation technique.* This technique was introduced by Shoenberg and Stiles (1964) and makes use of the extreme stability of superconducting magnets in their superconducting mode of operation. In this method, the specimen is placed inside a superconducting solenoid (giving, typically, fields up to 50 to 100 kG). When the current in the solenoid has been raised to a suitable value, the value of the current is made to change quite slowly (in some applications the magnet is put in its superconducting mode to hold the field constant). An additional coil is then used to modulate the field in the specimen at quite low frequencies (operation down to, say, 60 c/s presents no difficulties). Since the susceptibility of the specimen is oscillatory, there is a non-linear response in the specimen; for convenience the second (or higher) harmonic of the input signal is picked up and amplified. From this response as a function of the applied field the period of the de Haas-van Alphen oscillations can be found.

Because the modulation frequency can be made so low, this method lends itself readily to high pressure measurements; the superconducting solenoid, the modulating coil and the pick-up coil can all be outside the high-pressure vessel, which need contain only the single crystal of the metal under study (see for example, O'Sullivan and Schirber, 1966; Melz, 1966b).

2. *High-field Magneto-resistance*

The oscillatory behaviour of the magnetic susceptibility known as the de Haas-van Alphen effect, just discussed, arises from the quantization of the electron orbits in a magnetic field. These oscillatory effects are observable if the mean free path of the electrons is sufficiently large or, differently expressed, if $\omega_c \tau > 1$. Here ω_c is the cyclotron frequency and τ is the relaxation time of the conduction electrons involved in the particular orbit considered.

Under these conditions many other properties show corresponding oscillatory effects; in particular the resistivity of the sample in high magnetic fields (the Shubnikov-de Haas effect — Shubnikov and de Haas, 1930) and the Ettinghausen-Nernst effect. Both of these

1. The output from the pick-up tube, along with a signal can then be photographed and subsequently be measured.

was introduced by Shoenberger due to the extreme stability of superconducting mode of operation. In the case of a superconducting solenoid (10 kG). When the current in the solenoid is at a certain value, the value of the current in the specimen at quite low fields (30 c/s presents no difficulties). This is oscillatory, there is a non-linear dependence on the field (or higher) and amplified. From this the period of the de Haas-van

Alphen effect can be made so low, this method can be used for measurements; the superconducting pick-up coil can all be out-put to contain only the single crystal specimen. O'Sullivan and Schirber,

magnetic susceptibility known as the de Haas-van Alphen effect, arises from the quantization of the electron energy levels in a magnetic field. These oscillatory effects are observed when the Fermi level of the electrons is sufficiently close to the Landau level $\omega_c > 1$. Here ω_c is the cyclotron frequency of the conduction electrons.

The properties show corresponding changes in the resistivity of the sample in the de Haas effect — Shubnikov-de Haas effect — Nernst effect. Both of these

have been used to study the Fermi surface under pressure. As in the de Haas-van Alphen effect the period of the oscillations as a function of $1/H$ measures the area of the extremal cross-section(s) normal to H .

In addition to this oscillatory effect in the magneto-resistance, the field dependence of the magneto-resistance for different directions of the applied field can be used to determine certain dimensions of the Fermi surface related to its topology. This method was used by Caroline and Schirber (1963) to look for changes in the Fermi surfaces of Cu and Ag under pressure. The main features of the method are as follows.

Lifshitz and Peschanshii (1958) have shown that multiply-connected (open) Fermi surfaces show very characteristic behaviour in magneto-resistance at high fields. In a closed Fermi surface all the electron orbits in an applied magnetic field are necessarily closed. In these circumstances the magneto-resistance $\rho(H)$ saturates at high fields. This is true provided that the metal is not a compensated metal, i.e., with equal numbers of electrons and holes. If the metal is compensated with a closed Fermi surface $\rho(H)$ varies as H^2 for all field directions (see Fawcett, 1964).

In an open Fermi surface it may be possible to find for certain field directions orbits that can, because of the topology of the surface, never close. For these directions $\rho(H)$ varies as H^2 , whereas in the others where only closed orbits can occur $\rho(H)$ saturates. Of the possible open orbits one kind (referred to by Chambers (1962) as type B open orbits) can occur in a whole region of angles around certain symmetry directions. The solid angles that enclose these directions that support open orbits thus show on a stereogram as the boundaries of two-dimensional *areas*. Type A open orbits can occur in *planes* of applied magnetic field so that their directions are represented by *lines* on a stereogram. The dimensions of these regions or lines can be found because sharp peaks in the magneto-resistance are observed when the applied field direction passes through a type A region or crosses a boundary of a type B region. $\rho(H)$ depends not only on the direction of the applied magnetic field but also on α , the angle between the direction of the open orbit and the direction of the electric current. In fact $\rho(H)$ varies as $H^2 \cos^2 \alpha$ in directions where open orbits are involved.

3. Oscillatory Ettinghausen-Nernst Effect

This method was used by Balain *et al.* (1960) in their work on the Fermi surface of Zn under pressure. The Ettinghausen-Nernst coefficient B_{EN} (see, e.g., Jan, 1957) is defined by the relationship:

$$B_{EN} = -E_y/H \left(\frac{\partial T}{\partial y} \right) \quad (3)$$

In this it is supposed that, with no current flowing in the x direction, a magnetic field, H , is applied along the z axis. A temperature gradient $\partial T/\partial y$ is established along the y axis, and an electric field E_y in the y direction is then observed (it is determined from the potential difference across the specimen in the y direction divided by the corresponding thickness of the specimen).

The oscillatory part of the coefficient B_{EN} arises from the quantization of the conduction electron orbits in the field, H , and their passage through the Fermi level as in the de Haas-van Alphen effect.

The oscillations are likewise periodic in $1/H$ and their period, P , is given by:

$$P = 2\pi e/A\hbar \quad (4)$$

where A is the extremal cross-sectional area of the Fermi surface normal to H .

4. The Fermi Surface of Zn under Pressure

A comparison of the results from these different methods as applied to Zn has been made by O'Sullivan and Schirber (1966) and is shown in Fig. 3. This refers to the extremal cross-sections of the needles in Zn with the magnetic field parallel to b_3 (see Fig. 4); it illustrates that the de Haas-van Alphen measurements are in very good agreement with those from the oscillatory magneto-resistance measurements of Schirber (1965). Both these sets of measurements used the helium gas technique. Moreover, the results from these measurements are strongly corroborated in two different ways:

- (a) The initial slope is in close agreement with that found by Balain *et al.* (1960) who used truly hydrostatic pressures transmitted by liquid helium. Moreover, O'Sullivan and Schirber themselves used the liquid-helium technique (up to 140 b) to check the pressure

(1960) in their work on the Ettinghausen-Nernst coefficient by the relationship:

$$\left(\frac{\partial T}{\partial y}\right) \quad (3)$$

at flowing in the x direction, axis. A temperature gradient and an electric field E_y in the y direction are produced from the potential difference V divided by the corresponding length l .

It arises from the quantization of the energy levels in the magnetic field, H , and their passage through the Landau levels (de Haas-van Alphen effect).

$$\quad (4)$$

area of the Fermi surface normal to the direction of the magnetic field.

different methods as applied by Schirber (1966) and is shown in Fig. 4; it illustrates that the results are in very good agreement with the pressure measurements of Schirber (1966) used the helium pressure cell. From these measurements are shown in Fig. 4.

with that found by Balain et al. (1966) at pressures transmitted by the helium pressure cell and Schirber themselves used the helium pressure cell (see Fig. 4 b) to check the pressure

variation of the needle cross-sections. They did this using the phase-shift† de Haas-van Alphen technique, which is possible when the pressure can be varied continuously without upsetting the other experimental conditions (in particular, the temperature).

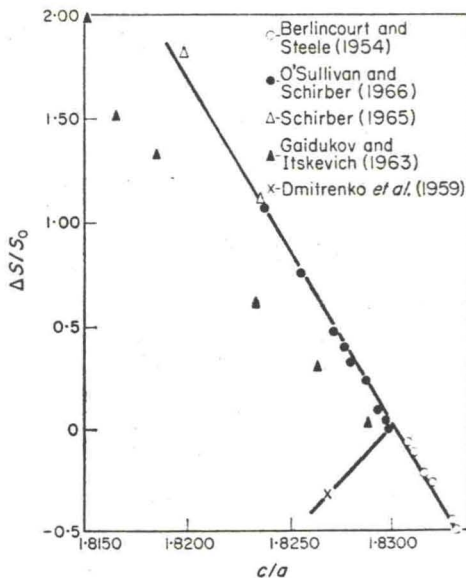


FIG. 3. Change in extremal cross-section for needles in Zn as a function of c/a ratio (After O'Sullivan and Schirber, 1966.)

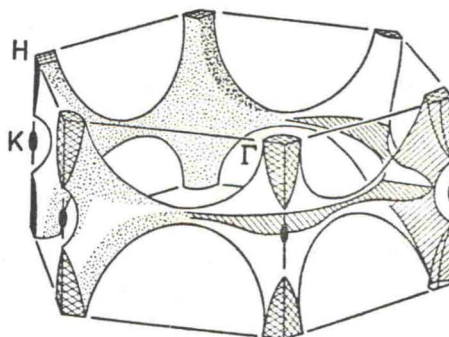


FIG. 4. Part of the Fermi surface of Zn. The "needles" are the black ellipsoids in the middle of the hexagon edges. (From O'Sullivan and Schirber, 1966.)

(b) The results of the pressure measurements form a smooth continuation to smaller values of c/a of the data obtained by Berlincourt and Schirber (1966).

† For a description of this technique, see Section III D5 on noble metals.

and Steele (1954).† In the latter experiments the c/a ratio changed simply because of the temperature change at constant (approximately atmospheric) pressure. As we shall see below, the almost totally predominating factor that determines the cross-sectional area of the needles is the c/a ratio. The results for the initial slope of the S_1 - P curve are summarized in Table II.

TABLE II. Extremal cross-sectional area as a function of pressure in Zn (needles with field parallel to b_3)

$\partial \ln S_1 / \partial P$	Observer
$32.0 \pm 1.5 \times 10^{-2} b^{-1}$	O'Sullivan & Schirber (1966)
$32 \pm 6 \times 10^{-2} b^{-1}$	Balain <i>et al.</i> (1960)
$30 \pm 3 \times 10^{-2} b^{-1}$	O'Sullivan & Schirber (1966)
$12 \pm 3 \times 10^{-2} b^{-1}$	Gaidukov & Itskevich (1963)

We can therefore conclude that the consistency between these different sets of experiments demonstrates that the helium gas technique gives reliable and reproducible results. We see, however, in Fig. 3 that the results obtained by the ice-bomb technique and by the oil-kerosene technique do not agree with each other or with the helium technique. The ice-bomb results are particularly notable because they give the wrong *sign* for the effect. Melz (1966a) (see also O'Sullivan and Schirber) has suggested that this effect can be understood as follows. In cooling the Zn crystal embedded in ice from the high temperature where the pressure is first generated, the crystal, because of its anisotropic properties, contracts more in the c than in the a direction. Because the ice cannot readily flow to compensate for this, the pressure in the c direction is reduced relative to that in the a direction. Thus the c/a ratio is *increased* instead of decreased as it would have been under hydrostatic pressure. Similarly, as both O'Sullivan and Schirber (1966) and Melz (1966a) point out, effects of this sort, but to a lesser degree, could account for the discrepancies in the measurements of Gaidukov and Itskevich (1963) using the oil-kerosene technique. More recent results at higher pressures (up to 15 kb) by Itskevich *et al.* (1965) indicate that at these higher values the pressure produced by this method may become more uniform and isotropic.

† In fact some re-interpretation of the data obtained by Berlincourt and Steele was needed.

iments the c/a ratio changed
ange at constant (approx-
shall see below, the almost
termines the cross-sectional
e results for the initial slope
Table II.

ea as a function of
ield parallel to b_3

Observer

& Schirber (1966)
L. (1960)
& Schirber (1966)
& Itskevich (1963)

sistency between these differ-
at the helium gas technique
We see, however, in Fig. 3
b technique and by the oil-
h other or with the helium
cularly notable because they
(1966a) (see also O'Sullivan
ct can be understood as fol-
n ice from the high tempera-
l, the crystal, because of its
the c than in the a direction.
pensate for this, the pressure
t in the a direction. Thus the
as it would have been under
Sullivan and Schirber (1966)
s sort, but to a lesser degree,
e measurements of Gaidukov
sene technique. More recent
by Itskevich *et al.* (1965) in-
pressure produced by this
isotropic.

btained by Berlincourt and Steele

Because Zn is so anisotropic in its thermal contraction, this exaggerates the non-hydrostatic effects of methods that rely on setting up the pressure in a solid at high temperatures. Presumably, these methods would not fail so badly with cubic materials, but as we saw earlier they may not be successful even then.

We have now seen something of the methods of measuring Fermi surfaces under pressure. Let us now see what physical understanding we can get from the results. A very important clue to our understanding of several metals that have been investigated (e.g., Zn, Al, Pb, In) is obtained from the nearly-free-electron model of the Fermi surface. We shall therefore consider this before looking at the experimental results in detail.

B. NEARLY-FREE-ELECTRON MODEL FOR ZN

If we have a gas of free electrons (i.e., independent electrons moving in a uniform potential), the energy of an electron of momentum p or wavenumber k is just $p^2/2m$ or $\hbar^2 k^2/2m$ where m is the electron mass. If the electrons form a completely degenerate gas, all the energy levels up to a certain energy, E_F , are occupied (each level with two electrons of opposite spin) and those above E_F are empty. The surface in k space that separates the occupied from the unoccupied region is called the Fermi surface and so for free electrons it is just a sphere:

$$\frac{\hbar^2}{2m} (k_x^2 + k_y^2 + k_z^2) = E_F \tag{5}$$

The radius of the sphere thus depends on E_F , i.e., on the number of electrons to be accommodated and on the volume available to them.

If we ignore the lattice potential inside a metal, and interactions between the electrons, then in this simple approximation the Fermi surface of the metal is a sphere in k space whose volume is just sufficient to accommodate all the valence electrons of that metal. If the metal has N atoms in volume V with z valence electrons per atom then:

$$E_F = \left(\frac{3}{\pi}\right)^{\frac{2}{3}} \frac{\pi^2 \hbar^2}{2m} \left(\frac{zN}{V}\right)^{\frac{2}{3}} \tag{6}$$

where we have allowed for two electrons of opposite spin per translational energy level. Thus E_F varies inversely as two thirds power

of the volume. Moreover, the Fermi radius k_F is related to E_F by the relation:

$$E_F = \hbar^2 k_F^2 / 2m \quad (7)$$

so that k_F varies as $V^{-1/3}$, i.e., inversely as the interatomic distance. Thus the simplest effects of pressure on the Fermi surface would be to increase the Fermi energy and Fermi radius.

So far we have ignored the effect on the conduction electrons of the periodic potential inside the lattice. If the interaction of the electrons with the lattice potential is very weak, it makes itself felt only when the periodicity of the lattice in a particular direction coincides with or is a multiple of the periodicity of the electron wavelength propagating in that direction. On this basis the Brillouin zone structure of the lattice is built up. If, in k space, the k vector of a conduction electron reaches from the centre of the Brillouin zone to a point on the zone boundary then that electron satisfies the Bragg condition for reflection by the set of lattice planes associated with the particular zone boundary. Within a given zone, the surfaces of constant energy must be continuous; only at the boundaries of the zone can discontinuities appear. Thus, in the limit of a vanishingly small potential, the constant energy surfaces are still spheres with modifications to their connectivity at the Bragg-reflection planes. For this reason it is convenient to map back into the first zone all the fragments of the surface that overlap into the second zone; likewise for those fragments in the third zone and so on. In this way, each sheet of the Fermi surface, corresponding to each zone, forms a continuous surface when re-mapped. Harrison (1966) has devised a convenient method of doing this mapping and worked out the shapes of the various sheets of the Fermi surface (contributed by different zones) for various lattice structures with various numbers of valence electrons to the atom.

A simple illustration of the scheme is given in Fig. 5, which shows the nearly-free-electron model of the Fermi surface of a simple square lattice in two dimensions (cf. also Pippard, 1960). The reciprocal lattice is then also a square lattice. The Fermi surface is now a circle and the occupied region overlaps into the second Brillouin zone as seen in the *extended zone* scheme at (a). In (b), the first sheet or band (i.e., the occupied area in the first zone) is shown by itself unchanged; the second sheet or band, however, has now been re-mapped back into the first zone. This is called the *reduced zone* scheme and represents the

that the Brillouin zone in this case both changes *size* and changes *shape* under pressure. The extended Fermi surface remains, of course, spherical and its size changes in inverse proportion to the volume change of the metal. But because the Brillouin zone is changing shape, the lines of contact of the Fermi sphere with the zone boundaries are altered so that the sheets of the Fermi surface in the reduced scheme

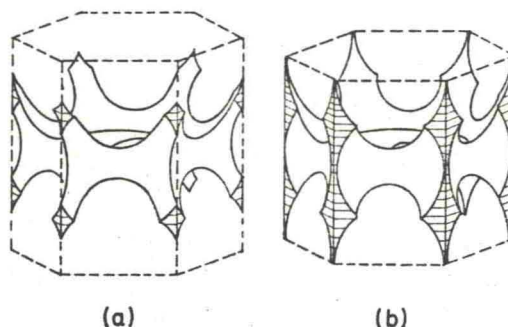


FIG. 6. The segment of the Fermi surface of a divalent hexagonal metal in the nearly-free-electron approximation: (a), corresponding to an axial ratio of 1.633; (b), corresponding to an axial ratio of 1.862. (From Harrison, 1965.)

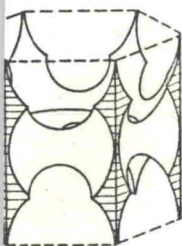
change in magnitude relative to each other (cf. Figs. 6a and b). Consequently we see that if pressure can alter the c/a ratio sufficiently, it can change the connectivity of the Fermi surface. Lifshitz (1960) predicted striking changes in the thermodynamic and transport properties of a metal at transitions where this connectivity is broken. The search for such effects has been one of the impulses behind the study of pressure effects in the hexagonal metals.

It is now clear how it is possible to calculate the changes in dimension of the different sheets of the Fermi surface of Zn when the c/a ratio changes, provided that the nearly-free-electron picture holds good. The geometry has been worked out in detail (Harrison, 1960; Higgins and Marcus, 1966) and the predictions for changes under pressure deduced. For example the extremal area of the needles when the magnetic field is parallel to b_3 is given by:

$$S_1 = \frac{4\pi}{9} \left(\frac{2\pi}{a} \right)^2 \left[\left(\frac{27\sqrt{3}z}{16\pi c/a} \right)^{\frac{1}{3}} - 1 \right]^2 \quad (8)$$

where now $Z = 2$ for zinc. (This expression is in the form given by Higgins and Marcus, 1966.)

h changes size and changes
i surface remains, of course,
e proportion to the volume
loun zone is changing shape,
with the zone boundaries are
urface in the reduced scheme



(b)

a divalent hexagonal metal in the
bonding to an axial ratio of 1.633;
(From Harrison, 1965.)

other (cf. Figs. 6a and b).
alter the c/a ratio sufficiently,
Fermi surface. Lifshitz (1960)
hydrodynamic and transport prop-
erties connectivity is broken. The
the impulses behind the study
etals.

calculate the changes in dimen-
sions of the Fermi surface of Zn when the c/a
nearly-free-electron picture holds
out in detail (Harrison, 1960;
predictions for changes under
extremal area of the needles
 b_3 is given by:

$$\left[\frac{\sqrt{3}z}{\pi c/a} \right]^{\frac{1}{3}} - 1 \quad (8)$$

expression is in the form given by

O'Sullivan and Schirber use this expression to derive the pressure derivative $\partial \ln S_1 / \partial P$. With the appropriate values of (c/a) and its pressure derivative, equation (8) yields a value for $\partial \ln S_1 / \partial P$ of $13 \times 10^{-2} \text{ kb}^{-1}$ compared with an experimental value of $32 \pm 1.5 \times 10^{-2} \text{ kb}^{-1}$. The authors emphasize, however, that the direct comparison must not be taken too seriously because of the *extreme* sensitivity of the result to small variations in the initial c/a value.

To make a more realistic comparison of the nearly-free-electron prediction, O'Sullivan and Schirber compare their result with measurements of changes in S_1 due to alloying by Higgins and Marcus (1966). On alloying, both the c/a ratio and the value of z (the number of valence electrons per atom) may change: in the pressure experiments, of course, only c/a changes. In their work, Higgins and Marcus found that on adding Cu to Zn, the value of $\partial \ln S_1 / \partial \ln \rho$ was 2.70×10^2 where $\rho = z/(c/a)$. O'Sullivan and Schirber note that the contribution to changes in S_1 from the factor a^2 in the denominator outside the square bracket in equation (8) is negligible. Consequently, S_1 depends essentially only on $z/(c/a)$, i.e., on ρ . Thus the pressure results can be compared directly with those from alloying; from the pressure results, O'Sullivan and Schirber deduce a value for $\partial \ln S_1 / \partial \ln \rho$ of 2.78×10^2 which is very close to the value deduced from the alloys.

In addition to these observations on the needles, O'Sullivan and Schirber made measurements on other characteristic dimensions of the Fermi surface of Zn. In general, they found qualitative agreement with the nearly-free-electron model; if allowance is made for discrepancies between this model and the true Fermi surface of Zn at atmospheric pressure, the agreement is within a factor of about 2. O'Sullivan and Schirber also made some rather more refined calculations (see Section III D 3).

Measurements of effective mass, m_c^* , were also made on Zn to determine how m_c^* changes with pressure. The cyclotron mass is defined in relation to ω_c the cyclotron frequency as follows:

$$\omega_c \equiv \frac{e}{m_c^*} H \quad (9)$$

ω_c measures the angular frequency with which an electron executes the particular orbit concerned when the applied field is H . In de Haas-van Alphen measurements this will be an extremal orbit.

Measurements of m_c^* are very valuable because they give a measure of the velocity associated with the particular orbit. This may be seen as follows. The equation of motion of an electron of wavenumber k in a magnetic field H is:

$$\frac{dk}{dt} = evH \quad (10)$$

where v is the component of the velocity of the electron normal to H and k changes in a direction at right angles to both v and H . Thus the electron moves in an orbit on the Fermi surface in a plane normal to H . The time taken to complete an orbit is thus, from equation (10):

$$T = \oint \frac{dk}{evH} = \frac{l}{eH \langle v \rangle} \quad (11)$$

where l is the perimeter of the orbit and $\langle v \rangle$ is the harmonic mean of the velocity round the orbit. Thus:

$$\omega_c = \frac{2\pi}{T} = \frac{eH 2\pi \langle v \rangle}{l} \quad (12)$$

and by comparison with the definition (9):

$$m_c^* = \frac{l}{2\pi \langle v \rangle} \quad (13)$$

Thus if we know m_c^* for a sufficient number of orbits, we can in principle find out how v varies over the Fermi surface.

We can use equation (13) to find out how m_c^* should change with pressure on the nearly-free-electron model. According to this model, l , the perimeter of an orbit, must be proportional to S where $S^{1/2}$ is the area of the orbit in k space (under pressure the orbits do not, except at certain singularities, change shape but only size). Thus from equation (13):

$$\frac{d \ln m_c^*}{dP} = \frac{1}{2} \frac{d \ln S}{dP} - \frac{d \ln \langle v \rangle}{dP} \quad (14)$$

Now the velocity, v , is the same all over the Fermi surface in the

because they give a measure of the angular orbit. This may be seen from the electron of wavenumber k in

$$(10)$$

of the electron normal to H at angles to both v and H . Thus the Fermi surface in a plane normal to the orbit is thus, from equation

$$\frac{l}{eH \langle v \rangle} \quad (11)$$

and $\langle v \rangle$ is the harmonic mean of

$$\frac{2\pi \langle v \rangle}{l} \quad (12)$$

$$(9): \quad (13)$$

number of orbits, we can in principle find the Fermi surface.

At how m_c^* should change with pressure. According to this model, m_c^* is proportional to S where $S^{1/2}$ is the surface area of the orbits do not, except at very low pressure (only size). Thus from equation

$$\frac{d \ln \langle v \rangle}{dP} \quad (14)$$

over the Fermi surface in the

approximation we are using here and is just proportional to k_F , i.e., to $V^{-1/3}$ where V is the volume of the metal. Thus:

$$\frac{d \ln m_c^*}{dP} = \frac{1}{2} \frac{d \ln S}{dP} - \frac{1}{3} \chi \quad (15)$$

where $\chi = -\frac{1}{V} \left(\frac{\partial V}{\partial P} \right)_T$, the isothermal compressibility of the metal.

O'Sullivan and Schirber tested this relation by measuring both the change with pressure of m_c^* and of S (as we have seen) for the extremal needle orbits normal to b_3 . They found:

$$\frac{d \ln m_c^*}{dP} = 14 \times 10^{-2} \text{ kb}^{-1}$$

compared to:

$$16 \times 10^{-2} \text{ kb}^{-1} \text{ for } \frac{1}{2} \frac{d \ln S}{dP}$$

(The second term on the right hand side of equation (15) is negligible). This again illustrates the value of this very simple, nearly-free-electron model of the Fermi surface.

We now turn to the results on cubic metals, such as aluminium and lead. Before doing so, however, we must see how the theory can be extended to cope with the more subtle changes in the Fermi surface under pressure in cubic materials where the approximation we have used hitherto would predict only a simple scaling effect.

C. THE PSEUDO-POTENTIAL METHOD

The general philosophy behind the pseudo-potential method (for a detailed account, see for example, Harrison, 1966) is that the forces on an electron inside an ion core are (1) a large attractive interaction with the nucleus and (2) a complicated interaction that arises from the presence of the other occupied electron orbitals about the nucleus. In some cases the second part can be considered to be derived from a repulsive potential (the pseudo-potential) which largely offsets the attractive potential corresponding to the first force. There thus remains a small effective potential which can be treated by standard methods, for example, by perturbation theory.

The pseudo-potential method in its complete form results from a transformation of the Schrodinger equation applied to the lattice potential, $V(r)$, and is exact. In the transformation, the ordinary lattice potential, $V(r)$, is as we saw replaced by a weak effective potential part of which arises from the pseudo-potential. This in its full generality, is a non-local integral operator, containing exchange terms and terms that arise from the orthogonalization of the crystal wave function to the occupied ion core electron states. The method becomes particularly useful if:

- (a) The pseudo-potential integral operator can be treated as essentially a simple potential.
- (b) The Fourier expansion of the resultant effective potential requires only a few terms corresponding to small reciprocal lattice vectors for its accurate representation.

In the above description I have used the term "pseudo-potential" to refer to the repulsive part of the interaction that offsets the attractive interaction with the nucleus. The resultant interaction I have called the "effective" interaction. This seems to have been the original usage, but it is now common to refer to the *resultant* potential as the pseudo-potential and so I shall do so from now on.

The result of replacing the actual potential inside the crystal by the weak pseudo-potential is that now the problem to be solved in finding the band structure of the metal is formally equivalent to that of the nearly-free-electron model of a metal.

Let me briefly remind the reader of how a simple one-dimensional calculation of this kind is carried out (Mott and Jones, 1936, p. 61). In a periodic lattice of lattice spacing a , the solution of the Schrodinger equation:

$$\frac{d^2 \psi}{dx^2} + \frac{2m}{\hbar^2} (E - V) \psi = 0 \quad (16)$$

is a Bloch function:

$$\psi = e^{ikx} u(x)$$

where $u(x)$, like $V(x)$, is periodic with the period a . Let us expand $u(x)$ in a Fourier series:

complete form results from a transformation applied to the lattice transformation, the ordinary potential is replaced by a weak effective pseudo-potential. This in its full form contains exchange terms and the localization of the crystal wave states. The method becomes

$$u(x) = \sum_{n=-\infty}^{\infty} A_n e^{-2\pi i n x/a} = \sum_{n=-\infty}^{\infty} A_n e^{-i K_n x} \tag{17}$$

where $K_n \equiv \frac{2\pi n}{a}$. Suppose for simplicity that apart from the constant term, A_0 , only one Fourier component K_1 is important; we then have:

$$\begin{aligned} \psi &= e^{i k x} (A_0 + A_1 e^{-i K_1 x}) \\ &= A_0 e^{i k x} + A_1 e^{i k_1 x} \quad \text{where } k_1 = k - K_1 \end{aligned} \tag{18}$$

Substituting this solution in the Schroedinger equation we find:

$$A_0 e^{i k x} \left\{ -k^2 + \frac{2m}{\hbar^2} (E - V) \right\} + A_1 e^{i k_1 x} \left\{ -k_1^2 + \frac{2m}{\hbar^2} (E - V) \right\} = 0 \tag{19}$$

If we multiply by $e^{-i k x}$ and integrate from 0 to a , we get:

$$\begin{aligned} -A_0 k^2 a + \int_0^a \frac{2m A_0}{\hbar^2} (E - V) dx \\ - \int_0^a \frac{2m A_1}{\hbar^2} e^{-i K_1 x} V dx = 0 \end{aligned} \tag{20}$$

We choose our origin of energy so that the mean value of V vanishes, i.e.:

$$\int_0^a V(x) dx = 0 \tag{21}$$

Thus we have:

$$A_0 (E - T_0) - A_1 V_1^* = 0 \tag{22}$$

Similarly by multiplying by $e^{-i k_1 x}$ and integrating we find:

$$-A_0 V_1 + A_1 (E - T_1) = 0 \tag{23}$$

Here:

$$T_0 = \frac{\hbar^2 k^2}{2m}$$

and:

$$T_1 = \frac{\hbar^2 k_1^2}{2m}$$

(the free-electron kinetic energies corresponding to the values k and k_1):

tor can be treated as essen-

tant effective potential re-
g to small reciprocal lattice
tion.

the term "pseudo-potential"
ction that offsets the attrac-
tant interaction I have called
have been the original usage,
tant potential as the pseudo-
on.

tial inside the crystal by the
oblem to be solved in finding
lly equivalent to that of the

ow a simple one-dimensional
tott and Jones, 1936, p. 61).
the solution of the Schroedin-

$$\psi = 0 \tag{16}$$

period a . Let us expand $u(x)$

$$V_1 = \frac{1}{a} \int_0^a V(x) e^{iK_1 x} dx$$

i.e., the Fourier component of the potential with period $1/a$.

To find E , we must eliminate A_0 and A_1 from equations (22) and (23). In this way, we obtain:

$$(E - T_0)(E - T_1) - V_1 V_1^* = 0 \quad (24)$$

which gives:

$$E = \frac{1}{2} [T_0 + T_1 \pm \sqrt{(T_0 - T_1)^2 + 4V_1 V_1^*}] \quad (25)$$

The resultant E - k curve is plotted in Fig. 7; it is of the familiar form with energy gaps whenever the wavenumber of the electron coincides with, or is a multiple of, the periodicity of the reciprocal lattice. When $k = k_1$ so that $T_0 = T_1$, it follows from equation (25) that:

$$E = T_1 \pm |V_1| \quad (26)$$

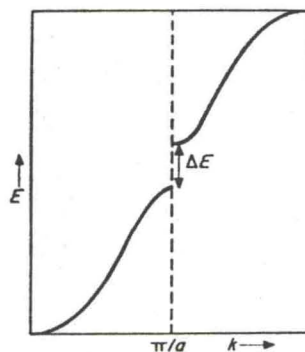


FIG. 7. E - k relation for nearly-free-electrons.

This specifies the range of forbidden values of E and the width of the energy gap is thus:

$$\Delta E = 2 |V_1| \quad (27)$$

Consequently the energy gap is determined by twice the corresponding Fourier component of the potential.

$\int_0^a \psi^2 dx$

potential with period $1/a$.

A_1 from equations (22) and

$$\int_0^a V_1^* \psi^2 dx = 0 \tag{24}$$

$$T_1^2 + 4V_1 V_1^* \int_0^a \psi^2 dx = 0 \tag{25}$$

Fig. 7; it is of the familiar form. The wavenumber of the electron k is a function of the energy E . The periodicity of the reciprocal lattice K_g follows from equation (25) that:

$$k = K_g + k' \tag{26}$$



free-electrons.

values of E and the width of the

$$\tag{27}$$

is increased by twice the corresponding

The above reasoning is easily generalized to three dimensions. The critical values of k are then those on the walls of the Brillouin zone. If k is close to a (111) face (in, say, an f.c.c. metal) then the Fourier component V_{111} will be important. At the centre of this face this component may suffice to determine the energy gap. Along the edge of a zone where two faces meet (say the 111 and 200 zone faces of an f.c.c. metal) then V_{111} and V_{200} may become important. At a corner, three Fourier components may be required. This illustrates how the Fourier components of the potential enter into the band-structure calculations. In addition we may note for future reference that in the neighbourhood of a zone face we may expect that at least two plane waves will be needed to specify the wave function of the electron, viz.:

$$e^{-i k r} \text{ and } e^{-i(k+K_g)r}$$

where K_g is the reciprocal lattice vector associated with that zone face.

All this is, of course, well known. What is new is its justification by pseudo-potential theory in relation to at least some real metals.

The method is particularly useful for constructing a Fermi surface from de Haas-van Alphen data. Where the model is most useful is, as we have seen, where only a few Fourier components of the pseudo-potential are significant. These (together with the Fermi energy) can then be taken as parameters and chosen to give the best fit with experiment in certain regions of the Fermi surface. Then the model can be used to calculate the rest of the Fermi surface and the band structure of the metal in the neighbourhood of Fermi energy. This phenomenological programme has, for example, been successfully carried out for Pb by Anderson and Gold (1965) (where, however, the situation is complicated by the strong spin-orbit coupling) and for Al by Ashcroft (1963).

The derivation of the Fermi surface, expressed in terms of a few Fourier coefficients of the effective potential, does not by itself enable us to predict what would happen to the surface under pressure. These Fourier coefficients, V_{111} and V_{200} , say, are valid for one particular value of the Fermi energy, and hence for one particular value of the lattice parameter only (that corresponding to zero pressure). To make any predictions about pressure effects, we need to know how V_{111} , V_{200} and E_F change when the lattice parameter alters, thus changing, among other things, the relative separations of the reciprocal lattice

points. We must therefore extend the model; this has been done by Harrison and others and we now consider this extension.

So far we have seen that if there exists a weak pseudo-potential that can be treated by perturbation theory we have a valuable phenomenological method for interpolation and for correlating experimental data about the Fermi surface. Now, however, we would like to know something about this potential from a rather more fundamental point of view. In particular, we want to know how to calculate the Fourier components of the potential or, more generally, its matrix elements between plane wave states. In this outline, we follow Harrison (1965, 1966).

We begin by assuming that there exists in the crystal a weak local effective (or pseudo) potential, $W(\vec{r})$, at each point. We then assume that this total pseudo-potential can be represented as the linear superposition of the individual ionic pseudopotentials centred on the ion sites. Thus:

$$W(r) = \sum_j w(|\vec{r} - \vec{r}_j|) \quad (28)$$

where the \vec{r}_j represent the positions of the N ions in the crystal, j going from 1 to N . This is a most important assumption and we shall discuss it below when we consider in more detail the nature of W itself. For the present, however, the point is that *if* this linear superposition holds then the matrix element of $W(\vec{r})$ (between states k and $k + q$) can be expressed as a product of two factors thus:

$$W(q) = S(q) w(k, q) \quad (29)$$

where:

$$w(k, q) = \frac{1}{V_0} \int e^{-i(k+q)r} w(r) e^{ikr} d\tau$$

is the matrix element of $w(r)$ between plane wave states k and $k + q$. $w(k, q)$ is called the *form factor*; it is independent of the positions of the ions and depends only on the ionic pseudo-potential. V_0 is here the atomic volume.

If $w(r)$ is a simple potential then the k dependence in the two exponential factors in $w(k, q)$ cancels out and $w(q)$ is in this case just the Fourier transform of $w(r)$. For our present purposes this simpler form is sufficient.

The factor $S(q) = \frac{1}{N} \sum e^{-iqr_j}$ is called the *structure factor*; by contrast with $w(k, q)$, it depends only on the positions of the ions. For a

model; this has been done by this extension.

A weak pseudo-potential that has a valuable phenomenological correlating experimental data, we would like to know a more fundamental point of view to calculate the Fourier potential, generally, its matrix elements, we follow Harrison (1965),

in the crystal a weak local potential at each point. We then assume the potential is presented as the linear superposition of potentials centred on the ion

$$V(\vec{r}) = \sum_j V_j(|\vec{r} - \vec{r}_j|) \quad (28)$$

the N ions in the crystal, j is an arbitrary point assumption and we shall give more detail the nature of W it is that if this linear superposition of $W(\vec{r})$ (between states k and k') can be written as two factors thus:

$$W(k, k') = W_1(k, k') W_2(k, k') \quad (29)$$

$$w(r) = \int e^{ikr} d\tau$$

plane wave states k and $k + q$. W is independent of the positions of the ions. V_0 is here the pseudo-potential.

The k dependence in the two exponential factors and $w(q)$ is in this case just the same. At this point we put this simpler form

the structure factor; by considering the positions of the ions. For a

perfect lattice at the absolute zero, it vanishes everywhere except at the reciprocal lattice points where it has the value unity.

This factorization into a structure factor and a form factor, characteristic of diffraction theory, is vital here.

We turn now to the calculation of the effect of volume on the Fermi surface. One way to obtain such information is to make a calculation using the full pseudo-potential theory, essentially a full orthogonalized plane wave (OPW) calculation, at two different volumes. However, there are simpler, though of course less exact, methods; one is to use Harrison's "point ion" approximation. In this, $w(q)$ is derived by representing the effective potential as made up of three contributions:

- (1) The coulomb potential due to the valence charge on the ion.
- (2) A repulsive term (originally referred to as the pseudo-potential) arising from the core electrons. As already discussed, the conduction electrons are to some extent excluded from the core because of the Pauli principle and because these inner shells are already occupied.
- (3) The potential due to screening by the conduction electrons. Because the conduction electrons in the metal are mobile they move to regions of low potential and thus partly screen the bare potential that the electrons would otherwise see; thus a self-consistent procedure is required. Such a procedure was introduced by Bardeen (1937) in his work on electron-phonon interaction in metals. For a free, degenerate electron gas of Fermi radius, k_F , the screening can be represented by an effective dielectric constant of which the Fourier component of wave-number q is:

$$\epsilon(q) = 1 + \frac{m e^2}{2\pi k_F \hbar^2 \eta^2} \left[\frac{1 - \eta^2}{2\eta} \ln \left| \frac{1 + \eta}{1 - \eta} \right| + 1 \right] \quad (30)$$

where $\eta = q/2k_F$. Here m and e are the mass and charge of the electron. Under these conditions, the ratio of $w_b(q)$, the bare potential, to $w_s(q)$, the self-consistent screened potential, is just $\epsilon(q)$. It is in part the simplicity of this self-consistent screening that makes it possible to represent the total crystal potential as the linear superposition of the individual ion potentials.

In the point ion model, the repulsive potential in (2) above is represented by a δ function (the ion core is considered as a point). If the

strength of the δ function is β then the form factor can be represented by:

$$w(q) = \frac{-(4\pi ze^2/q^2) + \beta}{V_0 \epsilon(q)} \quad (31)$$

where V_0 is the atomic volume.

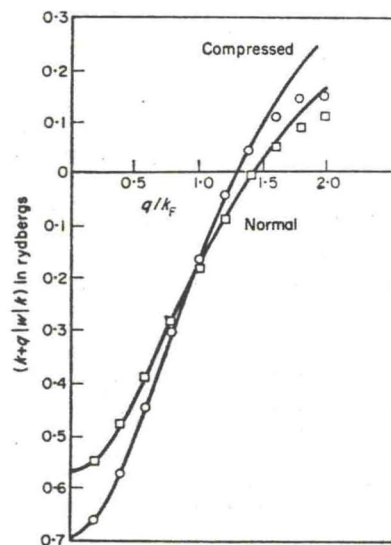


FIG. 8. Form factors for Al at normal volume and for lattice spacing reduced by 10%; the points are computed from the full pseudo-potential theory, and the curves correspond to results calculated from the model form factor. (From Harrison, 1965.)

An illustration of such a form factor is given in Fig. 8. This is as calculated by Harrison for Al at two different atomic volumes, the normal volume and that corresponding to a 10% reduction in lattice parameter. In the Figure the points have been calculated from the full pseudo-potential theory whereas the lines are derived from the simplified form factor expressed in equation (31). In the second derivation both z ($= 3$ for Al) and β are constant. The parameters that change with pressure are V_0 , k_F and hence $\epsilon(q)$. Thus apart from the volume itself the only change is in k_F , in the Fermi energy and hence in the screening.

We shall see below to what extent this simplified model, the point ion model, is successful in accounting for the effects of pressure on the

form factor can be represented

$$+ \beta \quad (31)$$



and for lattice spacing reduced pseudo-potential theory, and the model form factor. (From Harri-

Fermi surface of the simpler metals. The general procedure is to choose a model form factor (e.g., of the Harrison type) and choose the parameters involved in it so that this form factor will reproduce what is known experimentally about the Fermi surface of the metal at normal pressure. As an example, $w(q)$ for Al would have to take on the values V_{111} and V_{200} (as calculated by Ashcroft, say) when q is equal in magnitude to the corresponding reciprocal lattice vectors. Then the new form factor corresponding to a different volume can be deduced from the original one by suitably changing k_F and hence the values of $\epsilon(q)$.

Alternatively, the experimental results can be used to calculate how the important Fourier components of the pseudo-potential vary with volume. These values may then be compared with theoretical expectations.

In using a simplified version of the form factor, it should be remembered that because it has been chosen to fit the Fermi surface at a particular volume, this does not guarantee that it will be successful at a different volume even when the screening has been suitably altered. The simplified version of the form factor may contain unphysical assumptions that are concealed by the initial choice of parameters. The physically reasonable extrapolation to a different volume may then break down.

In what follows we shall compare theory and experiment for the metals Al, Pb and Zn. In this we shall essentially be considering to what extent a simplified form factor is successful in explaining the pressure dependence of certain features of their Fermi surfaces. We consider each of the metals in turn.

D. COMPARISON OF THEORY WITH EXPERIMENT

1. Fermi Surface of Al under Pressure

By way of illustration of the methods outlined above, let us consider first the Fermi surface of Al. The measurements by Melz (1966b) have already been referred to and we refer now to his calculations. These calculations were based generally on the calculations of the Fermi surface of Al made by Ashcroft (1963) which was itself an extension of earlier work by Harrison (1959, 1960).

is given in Fig. 8. This is as different atomic volumes, the to a 10% reduction in lattice ve been calculated from the e lines are derived from the ion (31). In the second deri- nstant. The parameters that ce $\epsilon(q)$. Thus apart from the the Fermi energy and hence

s simplified model, the point the effects of pressure on the

Following Melz, we concentrate our attention on the γ cross-section whose position is indicated in Fig. 9(a). It is the extremal orbit around the point U whose position in the Brillouin zone is illustrated in Fig. 9(b). In order to understand what happens to the area of this cross-section when the metal is compressed, we must look at the $E-k$

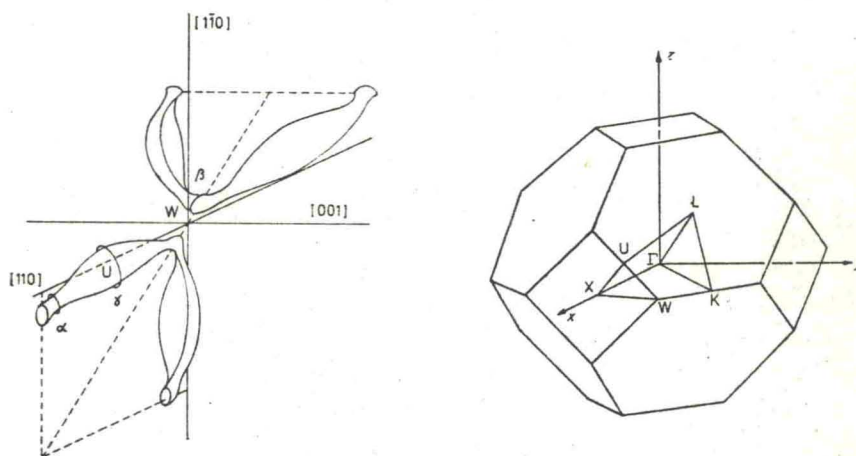


FIG. 9. (a). Part of the 3rd zone Fermi surface of Al. (From Melz, 1966b.) (b). First Brillouin zone of the f.c.c. structure showing labelling of some symmetry points.

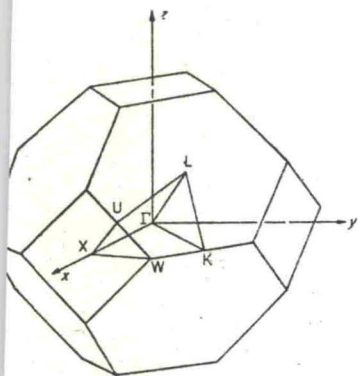
curves in the neighbourhood of the point U. The general form of the $E-k$ curves of Al in the specified symmetry directions as calculated by Ashcroft (1963) is illustrated in Fig. 10. The general form of these curves is quite similar to that for free electrons but with certain degeneracies removed by the effect of the weak pseudo-potential.

The inset of Fig. 10 shows the region around U and our attention is focussed on the highest of the 3 bands (U_3); in particular on whether this intersects the Fermi level. The Fermi level is also indicated in the diagram.

The γ oscillations are measured with the applied magnetic field in the [110] direction and two points on the corresponding extremal cross-section are indicated by A and B (Fig. 10). On going from U towards Γ (the centre of the zone) the $E-k$ curve reaches the Fermi level at A and on going from U towards X (the centre of the square zone face) the $E-k$ curve reaches the Fermi level at B.

The energy of the third band at U is given by:

ention on the γ cross-section is the extremal orbit around in zone is illustrated in Fig. ns to the area of this cross- we must look at the $E-k$



ce of Al. (From Melz, 1966b.) (b). wing labelling of some symmetry

t U. The general form of the etry directions as calculated 10. The general form of these e electrons but with certain e weak pseudo-potential.

around U and our attention (U₃); in particular on whether i level is also indicated in the

the applied magnetic field in the corresponding extremal (Fig. 10). On going from U $E-k$ curve reaches the Fermi s X (the centre of the square mi level at B. given by:

$$E_{U_3} = T_U + \frac{1}{2} \{V_{200} + (V_{100}^2 + 8V_{111}^2)^{\frac{1}{2}}\} \quad (32)$$

where T_U is the free-electron kinetic energy at U. The coefficients V_{200} and V_{111} have been referred to above; they may be thought of as Fourier components of the lattice pseudo-potential or as matrix ele-

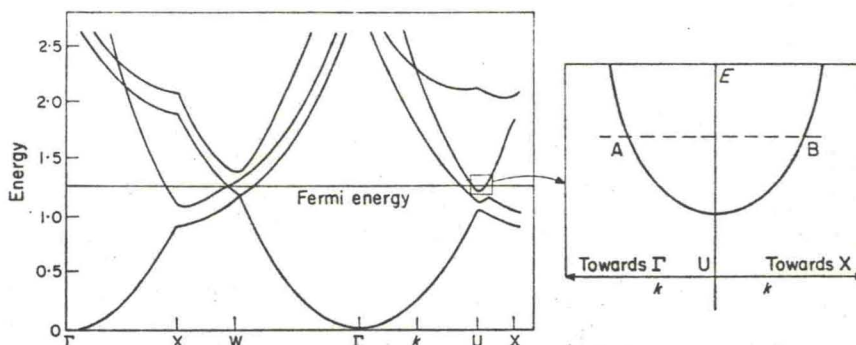


FIG. 10. Calculated band structure of Al (from Ashcroft, 1963). $E-k$ curves in the neighbourhood of the point U.

ments of the pseudo-potential taken between 2 orthogonalized plane waves differing by the reciprocal lattice vectors (200) and (111), respectively. V_{200} and V_{111} are positive. Moreover, Harrison (1965) has estimated that the pseudo-potential coefficients for Al should increase when the metal is compressed. Consequently, E_{U_3} would increase further above the free-electron value. Of course, both the free-electron kinetic energy and the Fermi energy would increase on compression, but these changes are small compared to the change in E_{U_3} (i.e., the energy splitting due to the pseudo-potential). The final result is that the whole third band is raised with respect to the Fermi energy and so, provided that the band retains its shape, the Fermi surface cross-section, γ (measured by the distance A-B in Fig. 10), will decrease under pressure.

To make a quantitative calculation of this effect, Harrison's model can be used in the manner indicated above to calculate the changes in the pseudo-potential due to pressure.

Melz carried out these calculations and found that a higher-order correction, arising from the next two higher energy levels, has a significant effect on the result. This higher-order effect can be put in without introducing new parameters. His results are shown in Fig. 11, and can be

compared with experiments. The Figure shows a comparison between the results (a) of the effectively free electron model (b) of the three OPW calculation without the higher order corrections and (c) of the three OPW calculations with higher-order corrections. The agreement of the latter with experiments is very good although the extreme

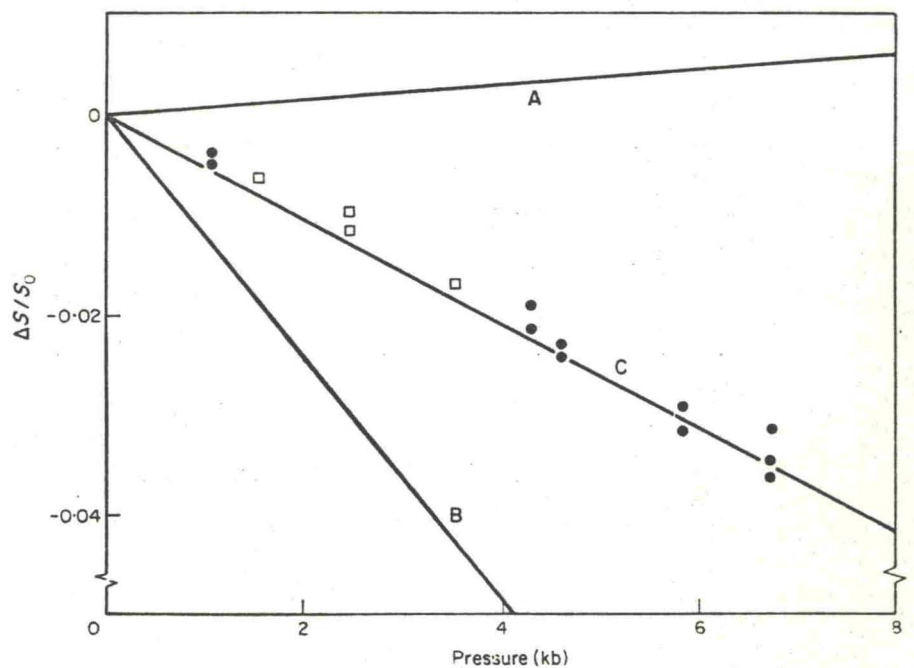


FIG. 11. The pressure dependence of the γ -[110] cross-section in Al. The points are the experimental results (two different samples). The lines represent theoretical calculations: A, simple scaling of the Fermi surface; B, calculation based on 3 OPW Ashcroft pseudo-potential; C, 5 OPW calculation. (From Melz, 1966b.)

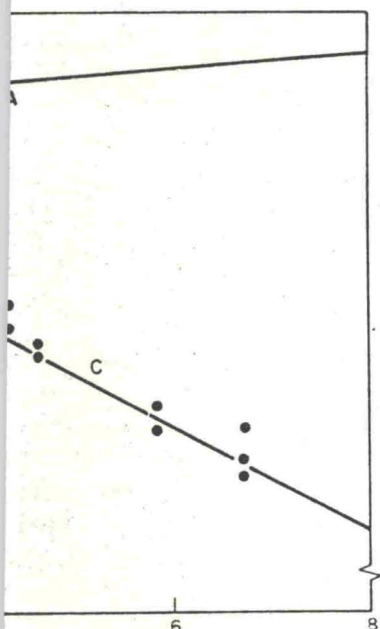
closeness is almost certainly fortuitous. For our present purposes, however, the point is that this sort of calculation can explain some of the features of the pressure dependence of the Fermi surface of Al.

Melz made further comparisons between experiment and theory, although the other cross-sections do not lend themselves so readily to theoretical comparison.

2. Fermi Surface of Pb under Pressure

Anderson *et al.* (1967) measured the effect of pressure on some extremal cross-sections of the Fermi surface of Pb and used their results to

shows a comparison between electron model (b) of the three order corrections and (c) of the first order corrections. The agreement is good although the extreme



[110] cross-section in Al. The points are experimental (circles). The lines represent theoretical calculations: A, calculation based on 3 order corrections; B, calculation based on 3 order corrections; C, calculation based on 1 order correction. (From Melz, 1966b.)

s. For our present purposes, the calculation can explain some of the features of the Fermi surface of Al. The agreement between experiment and theory, which does not lend themselves so readily

effect of pressure on some extremely low temperature of Pb and used their results to

estimate the variations with pressure of the appropriate Fourier coefficients of the pseudo-potential. They found also that model potential calculations correctly predicted the signs in the changes of V_{111} and V_{200} with pressure, although the magnitudes were wrong by a factor of 5 or so. They concluded that calculations using more exact forms for the potential were needed to make a satisfactory comparison between theory and experiment.

3. *Effect of Pressure on the Fermi Surface of Zn*

As already mentioned, O'Sullivan and Schirber improved their estimates of the pressure dependence of their S_2 cross-section by using a three-OPW calculation based on a model potential rather like Harrison's calculations on Al. Their model potential did not altogether agree with deductions made from de Haas-van Alphen data of the Fermi surface under zero pressure. They assumed, however, that it might yield reasonable derivatives for the purpose of calculating pressure coefficients. Their results agreed within a factor of 2 with their experiments.

There have recently been further measurements of In and Be and in general it appears that the pseudo-potential theory in its simpler forms can give at least a qualitative account of the pressure effects.

4. *The Monovalent Metals*

Considerable experimental work on the properties of the noble metals under pressure at low temperatures has been done, and so we shall first look at the effect of pressure on the Fermi surface of these metals before turning to the alkali metals.

5. *Experiments on the Noble Metals*

The shape of the Fermi surfaces of the noble metals is now well established by a wide range of experimental techniques (see for example Shoenberg, 1962, and Roaf, 1962).

The shape of the Fermi surface of a noble metal together with the first Brillouin zone is illustrated in Fig. 12. This shows that the Fermi surfaces of the noble metals touch the Brillouin zone boundaries on the hexagonal {111} zone faces. The area of contact increases in the sequence Ag, Au, Cu. The Fermi surface of Ag thus departs least from

that of a sphere, but in all of them, because of the contact with the zone boundary, the surfaces in the repeated zone scheme are multiply connected.

Where the Fermi surface contacts the zone boundary is usually referred to as the neck region; regions away from the necks are usually

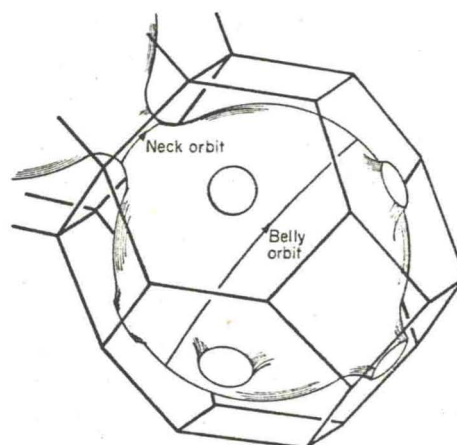


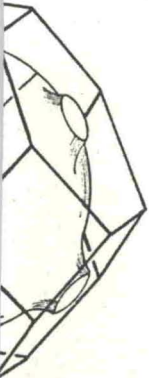
FIG. 12. First Brillouin zone and Fermi surface of a noble metal (schematic). The extremal belly and neck orbits with the magnetic field in the $[111]$ direction are shown.

referred to (following Shoenberg) as the bellies. As we shall see below there are important regions, particularly in gold, where the surface is significantly concave in the $\{110\}$ direction.

The first experiments seeking to find out how the Fermi surfaces of the noble metals changed under pressure were those of Caroline and Schirber (1963) who measured the transverse magneto-resistance at high fields to pick out the regions associated with open orbits. In this way they could measure the angular diameter of the necks in the Fermi surfaces of copper and silver from the angular separation of the corresponding peaks in the transverse magneto-resistance; they were thus able to concentrate directly on *distortion* of the Fermi surface, since if the whole surface and Brillouin zone simply scale together under pressure, the angular diameter of the necks does not change. The method of applying pressure was by means of the helium gas technique and they used pressures up to 2 kb. Their precision was such that they could detect changes of 0.2% per kb in Cu and 0.3% per kb in Ag. No changes were detected.

use of the contact with the
ed zone scheme are multiply

e zone boundary is usually
y from the necks are usually



face of a noble metal (schematic).
agnetic field in the [111] direction

bellies. As we shall see below
ly in gold, where the surface
ection.

out how the Fermi surfaces
essure were those of Caroline
transverse magneto-resistance
associated with open orbits. In
r diameter of the necks in the
the angular separation of the
magneto-resistance; they were
distortion of the Fermi surface,
in zone simply scale together
of the necks does not change.

by means of the helium gas
2 kb. Their precision was such
% per kb in Cu and 0.3% per

As we saw above, Shoenberg and Stiles (1964) introduced the modulation technique for measuring de Haas-van Alphen signals in conjunction with the use of a superconducting magnet to produce the magnetic field. In applying this method to determine the Fermi surfaces of the alkali metals they used a fixed field and rotated the specimen; in this way the signals measure directly departures of the surface from sphericity, thereby providing a very direct and sensitive technique for metals with nearly spherical Fermi surfaces. A further development came with the application of the method to determining how tension alters the Fermi surfaces of the noble metals (Shoenberg and Watts, 1965). In this work the strains involved were very small (10^{-3} or 10^{-4} , to remain within the elastic limit). The authors achieved a high enough sensitivity to measure the changes in cross-section of the Fermi surface by observing changes in the phase of the oscillation in a fixed field of about 50 kg. At this field the phase of the belly oscillations is about 10^4 and of the neck oscillations about 5×10^2 . Their apparatus was sensitive enough to detect a change of phase of about $1/10$ of an oscillation, thereby making possible a sensitivity and accuracy of about 1 part in 10^5 for the belly and 1 part in 5×10^3 for the neck oscillations.

The application of this method to measurements of the effect of pressure on the Fermi surface was made by Templeton (1966). He again used the sensitivity that comes from observing a phase change in a fixed field. In his apparatus he achieved a sensitivity of about 1 part in 10^7 for the belly oscillations. To measure distortions of the Fermi surface he compared directly the relative phase of belly and neck oscillations from the [111] direction. Because of the high sensitivity of the method, Templeton could use the hydrostatic pressure (up to about 25 atm) available with liquid helium at 1.2° K. Figures 13 and 14 illustrate the two aspects of this work. In Fig. 13 we see a sequence of steps that record the change in phase of the belly oscillations in gold in a persistent field of 50 kg. Each step corresponds to an increase or decrease of the pressure by about 3.5 b. Between each step the limits of the particular de Haas-van Alphen cycle have been checked by slightly perturbing the magnetic field (without, however, permanently changing the persistent current). The results obtained in this way were not entirely satisfactory, because to calibrate the changes in phase in terms of the change in area of orbit requires the assumption that the susceptibility oscillations are truly sinusoidal. A null method was therefore used in which the phase shift produced

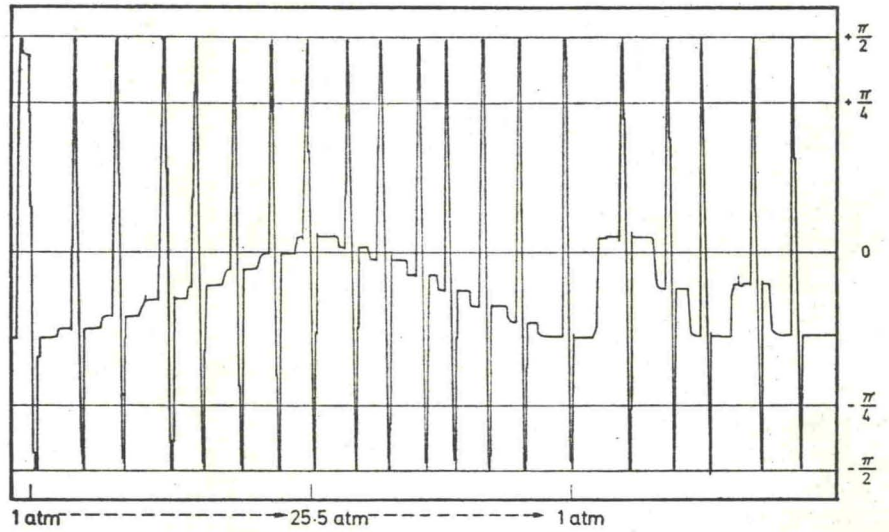


FIG. 13. Phase changes in the [111] belly oscillations of Au due to pressure changes. The applied field is about 50 kG. (From Templeton, 1966.)

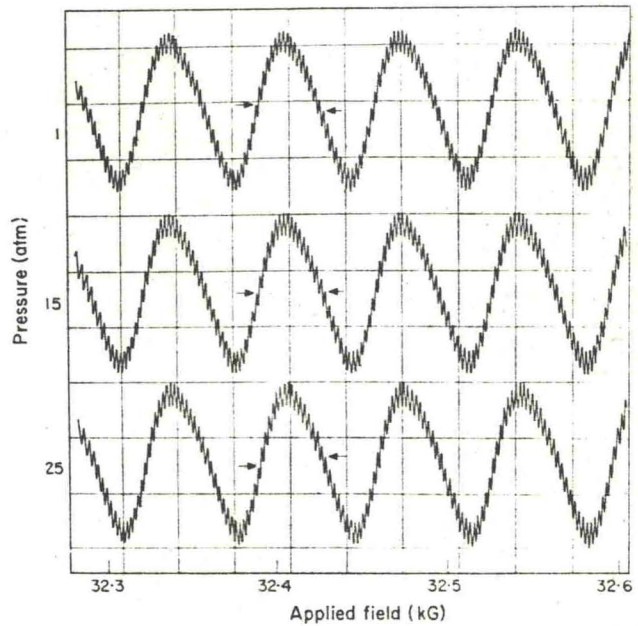
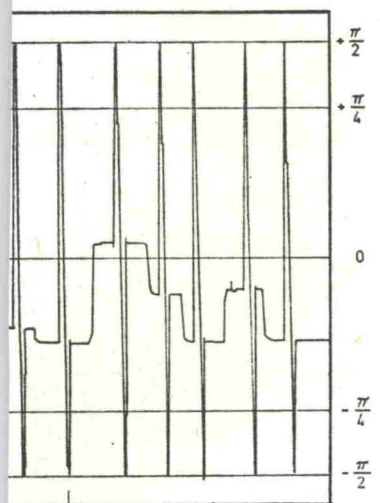
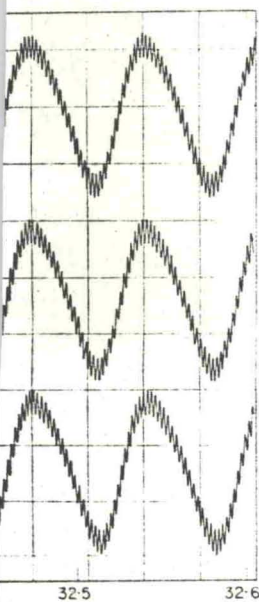


FIG. 14. Neck and belly oscillations in the [111] direction in the de Haas-van Alphen effect in Au at three different pressures. The arrows indicate corresponding belly oscillations and show the relative phase change with pressure. (From Templeton, 1966.)



oscillations of Au due to pressure (from Templeton, 1966.)



[111] direction in the de Haas-van Alphen effect. The arrows indicate corresponding change with pressure. (From Templeton, 1966.)

by the change of pressure was just offset by a suitable change in a supplementary source of magnetic field. The phase shift could then be calculated from the required field change.

In Fig. 14 we see how in Templeton's method the relative phase of belly and neck oscillations is compared at different pressures. In these measurements there is no change of phase with pressure as long as different parts of the Fermi surface just scale in the same proportion. The method thus detects directly *distortion* of the Fermi surface with pressure. In the Figure, the high-frequency oscillations arise from the belly and the low frequency oscillations from the necks. The arrows indicate one particular belly cycle; to follow its position without ambiguity it is necessary to make measurements at smaller pressure intervals than those illustrated in the Figure.

Once the relative phase change between the belly and neck oscillations has been determined, we can then find the relative changes in area as follows. The cross-sectional areas A_n of the allowed orbits of the electrons in a field H are given by:

$$A_n = 2\pi(n + \gamma) eH/\hbar \tag{33}$$

where γ is a phase factor that we assume remains constant and n is an integer. Now let N_N and N_B be the corresponding values of $n + \gamma$ for the neck and belly oscillations, respectively, at a given value of H :

Therefore:

$$\frac{N_N}{N_B} = \frac{A_N}{A_B} \tag{34}$$

where A_N and A_B are the cross-sectional areas of the extremal neck and belly orbits.

Consequently if we fix on a given neck orbit and so keep N_N constant but allow A_N and A_B to change because of the pressure, the change in N_B is given by:

$$-\frac{\Delta N_B}{N_B} = \frac{\Delta A_N}{A_N} - \frac{\Delta A_B}{A_B} \tag{35}$$

It is clear from this result that if the two orbits scale in the same proportion $\frac{\Delta A_N}{A_N} = \frac{\Delta A_B}{A_B}$ and $\Delta N_B = 0$. From the experiment on

the belly oscillations alone $\Delta A_E/A_B$ can be measured rather accurately, and so from the experiment that measures ΔN_B , $\frac{\Delta A_N}{A_N}$ can be accurately derived. Alternatively the relative change of cross-section $(\Delta A/A)_N - (\Delta A/A)_B$ may itself be the quantity desired.

Templeton's results for the three noble metals are summarized in Table III. They show that this provides a very accurate way of meas-

TABLE III. Change of anisotropy and Fermi surface with pressure

Metal	$\frac{\partial \ln \rho_{ph}}{\partial \ln V}$ (0° C)	γ	$\frac{d \ln K}{d \ln V}$	Change in elastic anisotropy with pressure $\left(\frac{d \ln A}{d \ln V}\right)^\dagger$	Distortion of Fermi surface with pressure
Li	-0.49	0.9	-2.3	-0.4	..
Na	4.6	1.3	2.0	0	..
K	5.6	1.3	3.0	0	Small
Rb	4.3	1.0	2.3
Cs	3.1	1.0	1.1
					$\left[\frac{d \ln r_N}{d \ln V}\right]$ distortion ‡
Cu	3.0	2.0	-1.0	-0.87	-1.1 ± 0.2
Ag	3.9	2.4	-0.9	-0.84	-2.1 ± 0.2
Au	5.5	3.1	-0.7	-2.1	-1.5 ± 0.2

$^\dagger A$ is the anisotropy parameter $2 C_{44}/(C_{11}-C_{12})$.

‡ This measures the distortion effect only; scaling effects have been subtracted.

uring essentially the pressure *derivative* of the different cross-sections at $P = 0$. In all three metals, pressure increases the area of contact at the zone boundaries, i.e., enhances the distortion of the Fermi surface. Since this was written further experimental work has been done on copper; see O'Sullivan and Schirber (1968), and Gerhardt (1968).

6. Experiments on the Alkali Metals

So far Templeton has made measurements on K under the pressures available with liquid helium. He has measured the relative change in area of orbits on several different and randomly oriented crystals. The changes correspond, within experimental error, to those to be expected from simple scaling of the Fermi surface to the relative change in the size of the unit cell.

be measured rather accurately. The relative change of cross-section quantity desired.

The metals are summarized in a very accurate way of meas-

Fermi surface with pressure

Change in elastic anisotropy pressure ($\frac{\Delta A_N}{A_N} - \frac{\Delta N_B}{N_B}$) [†]	Distortion of Fermi surface with pressure
-0.4	..
0	..
0	Small
..	..
..	..
	$\left[\frac{d \ln r_N}{d \ln V} \right]$ distortion [‡]
-0.87	-1.1 ± 0.2
-0.84	-2.1 ± 0.2
-2.1	-1.5 ± 0.2

C₁₂).
Coring effects have been subtracted.

of the different cross-sections increases the area of contact the distortion of the Fermi experimental work has been Pircher (1968), and Gerhardt

experiments on K under the pressures measured the relative change in randomly oriented crystals. experimental error, to those to be Fermi surface to the relative

7. Effect of Pressure on the Fermi Surfaces of the Monovalent Metals: Theory

The theoretical situation is very much the inverse of the experimental one. Detailed calculations of the effect of pressure on the band structure of the alkali metals have been made by Ham (1962); on the other hand very little work has been done on pressure effects in the noble metals although, of course, the band structure of Cu at atmospheric pressure has been studied in detail (see, for example, Segall, 1962, and Burdick, 1963). (But see added note on p. 141.)

8. The Alkali Metals

Ham's calculations were based on the quantum defect method in which the details of the electron-ion potential in the free state are fed into the calculation directly through the quantum defect parameters which characterize the atomic spectra of the elements. The main purpose of the calculations was to illustrate the trend in the band structures in going through the alkali metal series. This purpose is particularly apposite in the present context because Ham's results can be compared, as we shall see in the next Section, with experimental results on electrical resistivity for all the alkali metals and also with the outcome of some of the theoretical calculations of resistivity in the same group of metals.

The results of Ham's calculations are very detailed: they give the shapes of the Fermi surfaces, the electron velocities, density of states, indeed all the band structure information not only at atmospheric pressure but over a wide range of volumes.

It is not yet possible to compare Ham's predictions about the influence of pressure on the Fermi surface of the alkali metals directly with experiment, but it is possible to test his predictions about the shape of the Fermi surfaces at atmospheric pressure, since these (except for Li) are now well established experimentally (Shoenberg and Stiles, 1964; Okumura and Templeton, 1965).

This comparison shows that Ham's calculations consistently overestimate the distortions of the Fermi surface except in Na. In Na, Ham predicted, and experiment has since confirmed, that the Fermi surface is very nearly spherical. In going towards the heavier metals the distortion, according to Ham, should be increased in the sequence K, Rb, Cs. In Cs, the distortion should be so great that the Fermi sur-

face should be nearly touching the zone boundaries. Likewise in Li, distortion of the Fermi surface would be large and comparable to that in Cs. The experiments have shown that in K the Fermi surface is slightly more distorted than in Na though still very close to a sphere; the radial distortion is about 1 in 10^3 . In Rb, the distortion amounts to about 1% in radius and in Cs (Okumura and Templeton, 1965) to only about 5%. In lithium (Stewart *et al.*, 1964) the Fermi surface is known only from positron-annihilation experiments; these indicate a radial distortion, as in Cs, of about 5%. We see, therefore, that the calculations give the right trend of distortion among the alkali metals, although numerically the agreement is not too close. One might, therefore, expect a similar result for the pressure dependence: i.e., that Ham's predictions would be qualitatively correct, but might overestimate the effects. This would imply that the Fermi surfaces of Li and Cs would be particularly susceptible to change under pressure. So far, however, no experimental evidence on these two metals is available. As we shall see below, however, Ham's calculations have been used with some success to calculate changes of resistivity under pressure.

9. *The Noble Metals: Theory*

Segall's calculations of the Fermi surface of Cu at atmospheric pressure illustrated the importance of the low-lying fully occupied *d* band on the shape of the Fermi surface. Segall emphasized that the interaction between the *d* levels and the *sp* energy bands depends on the symmetry direction under consideration. It is particularly strong in the [110] directions. Where this interaction can occur its effect is illustrated in Fig. 15. From this Figure it is clear that if the Fermi level lies above the general average energy associated with the *d* levels, the effect of this interaction is to push the *E-k* curve of the *s* like electrons in towards the origin. This means that compared to the free electron sphere, the true Fermi surface of the noble metals tends to be pushed in in the [110] directions. Such concave areas around the [110] directions are indeed found; they are particularly conspicuous in Au and Cu. Since in the monovalent metals, one electron per unit cell has to be accommodated within the Fermi surface, this inward bulging

boundaries. Likewise in Li, large and comparable to that in K the Fermi surface is still very close to a sphere; Rb, the distortion amounts (Mara and Templeton, 1965) to (Ham, 1964) the Fermi surface is still very close to a sphere; these indicate a

We see, therefore, that the distortion among the alkali metals, is not too close. One might, therefore, expect a pressure dependence: i.e., that the Fermi surface is not too close, but might overestimate that the Fermi surfaces of Li and K are to change under pressure. The influence on these two metals is not clear, but Ham's calculations have shown that changes of resistivity under

implies that the surface must bulge out in some other directions. Because of the energy gap at the [111] zone faces and because these faces lie close to the undistorted Fermi sphere, the Fermi surface tends to bulge towards these faces. This, together with the [110] concavities, forces the Fermi surface actually to contact these [111] zone faces. It is significant that the area of contact is greatest in Cu, which has the highest d levels, next greatest in Au and least in Ag, which has the lowest lying d levels.

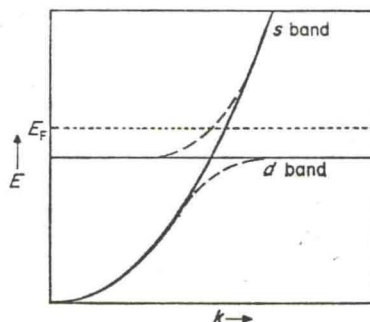


FIG. 15. The effect of interaction between s and d bands (schematic).

On this basis one may conjecture that the influence of pressure on the Fermi surface of the noble metals will make itself felt most strongly through the d electrons. On compressing the metal, the d bands would be expected to broaden in energy, and their mean energy to rise.† This will increase the effects of the interactions between sp like and d like energy bands, which in turn would exaggerate the distortion already referred to. Consequently one would expect that pressure would increase the areas of contact in the [111] directions and enhance the concave areas in the [110] directions. The experimental results of Templeton show that, at least as far as [111] directions are concerned, these ideas correspond with what is found experimentally. There have recently appeared some calculations of the effect of volume change on the Fermi surface of copper by Davis *et al.* (1968).

† A rough argument is as follows. Compressing the metal increases the overlap of the original atomic d orbitals. Consequently the d band will broaden on compression. A rise in the average band energy may be attributed to the increase on compression of the exponentially varying repulsion between the closed shells.

surface of Cu at atmospheric pressure. The low-lying fully occupied d bands. Segall emphasized that the energy of the sp energy bands depends on the direction. It is particularly strong interaction can occur its effect is illustrated by the fact that if the Fermi level lies close to the d levels, the effect of the s like electrons in noble metals tends to be pushed outwards around the [110] directions, particularly conspicuous in Au. In Cu, one electron per unit cell has a Fermi surface, this inward bulging

IV. EFFECT OF PRESSURE ON ELECTRICAL CONDUCTIVITY

We turn now to the problem of understanding how the electrical conductivity of a metal varies with pressure. We shall be concerned almost exclusively with the monovalent metals, i.e., the alkali metals on the one hand and the noble metals on the other. On the other hand, there have been recent important theoretical developments relating to the divalent metals (Vasvári and Heine, 1967; Vasvári *et al.*, 1967) stimulated largely by the experimental findings of Drickamer and co-workers (Stager and Drickamer, 1963; Drickamer 1965; see also the reviews by Lawson, 1956; Paul, 1963; and Landwehr, 1965).

A. PHONON-SCATTERING PROCESSES

As a preliminary, let us consider briefly some of the mechanisms that give rise to electrical resistivity in metals. The electric current is carried by the conduction electrons, of which in the monovalent metals there are just one per atom. These electrons form a highly degenerate electron gas whose Fermi energy can be estimated on the assumption that the conduction electrons form a free-electron gas confined within the volume of a metal. The Fermi energy therefore depends on the atomic volume of the metal and varies from about 80,000° K in Cu to about 20,000° K in Cs (both at normal pressure). We see therefore that even at room temperature the zero-point kinetic energy of the electrons is very large compared with a typical thermal energy kT .

At the absolute zero of temperature in a perfect lattice (i.e., a lattice free from physical or chemical imperfections) the conduction electrons may be thought of as waves propagating in a perfect periodic structure. Consequently they can travel without being scattered, and the metal would therefore have zero resistivity (this is not to be confused with the superconducting state which has quite different and distinct properties).

All real metals have some impurities or physical imperfections, including boundaries, that limit the conductivity of the metal in its non-superconducting state. The resistivity that remains at the lowest temperatures and is independent of temperature is called the residual resistivity, ρ_0 . For very pure perfect metals, it can be made a very small fraction of the room-temperature resistivity; typically, in such pure metals, the ratio of room temperature to residual resistivity may be 10^4 or more.

ELECTRICAL CONDUCTIVITY

Understanding how the electrical resistance varies with temperature is of great importance. We shall be concerned with the electrical conductivity of pure metals, i.e., the alkali metals and the noble metals, and compare it with the other. On the other hand, theoretical developments relating to the electrical conductivity (see, for example, 1967; Vasvári *et al.*, 1967) and experimental findings of Drickamer and co-workers (1963; Drickamer 1965; see also 1963; and Landwehr, 1965).

SCATTERING PROCESSES

Understanding the mechanisms of scattering of conduction electrons in metals is of great importance. The electric current is carried by conduction electrons which in the monovalent metals form a highly degenerate Fermi gas. The energy of the conduction electrons is estimated on the assumption of a free electron gas confined within a volume. The energy therefore depends on the volume (from about 80,000° K in Cu at normal pressure). We see therefore that the Fermi energy of the conduction electrons is of the order of a typical thermal energy kT . In a perfect lattice (i.e., a lattice with no impurities) the conduction electrons in a perfect periodic structure are scattered by phonons, and the metal resistance is not to be confused with the resistance due to impurities and lattice imperfections.

Understanding the mechanisms of scattering of conduction electrons in metals is of great importance. The electric current is carried by conduction electrons which in the monovalent metals form a highly degenerate Fermi gas. The energy of the conduction electrons is estimated on the assumption of a free electron gas confined within a volume. The energy therefore depends on the volume (from about 80,000° K in Cu at normal pressure). We see therefore that the Fermi energy of the conduction electrons is of the order of a typical thermal energy kT . In a perfect lattice (i.e., a lattice with no impurities) the conduction electrons in a perfect periodic structure are scattered by phonons, and the metal resistance is not to be confused with the resistance due to impurities and lattice imperfections.

The periodicity of the ideal lattice thus explains the vanishing of resistance in pure, perfect metals as the absolute zero is approached. The success of the picture in this respect has tended to focus attention on the periodic structure of metals even when their electrical conductivity at high temperatures is under consideration. As we shall see below, this is in some ways a mistaken approach and for high-temperature purposes this emphasis on the periodic lattice is not necessarily the most helpful.

In addition to the electrical resistivity that arises from the scattering of the conduction electrons by chemical impurities and physical imperfections there is also, at any temperature above the absolute zero, scattering due to the thermal vibrations of the lattice, i.e., to phonons. It is this scattering by phonons that gives rise to the temperature-dependent part of the electrical resistivity ρ_{ph} . As a first approximation we assume that the total electrical resistivity, ρ , at any temperature is given by:

$$\rho = \rho_{ph} + \rho_0 \quad (36)$$

This is known as Matthiessen's rule, and although a valuable generalization it is not strictly valid, and as we shall see below it can, in certain circumstances, give misleading information.

We turn now to a more detailed discussion of the scattering of electrons by phonons. Suppose that an electron of wavenumber k and energy E_k is scattered by absorbing a phonon of wavenumber, q , frequency ω and energy $\hbar\omega$ into a state k' of energy $E_{k'}$. Conservation of energy then requires that:

$$E_{k'} - E_k = \hbar\omega \quad (37)$$

We also require that:

$$k' - k = q + G \quad (38)$$

where G is a reciprocal lattice vector. This relationship is in some way analogous to conservation of momentum. When G is zero, we have a so-called normal process and when G is non-zero we have an Umklapp process. The Umklapp process (U-process, for short) can be interpreted in the following way. If $k' - k = G$, this means that the electron satisfies the Bragg condition for reflection from the lattice planes corresponding to the reciprocal lattice vector G ; consequently, we may think of the scattering process, described by the process above, as implying that the electron is scattered by a phonon of wavenumber q

and at the same time Bragg-reflected by the appropriate lattice planes.

U-processes are very important because they provide a means by which the momentum in the electron system can be communicated directly to the lattice as a whole. They therefore provide an immediate source of electrical resistivity. They are also important because G is a large vector and therefore even when q is small, U-processes make possible large angle scattering processes. This is particularly important at low temperatures (Bailyn, 1960).

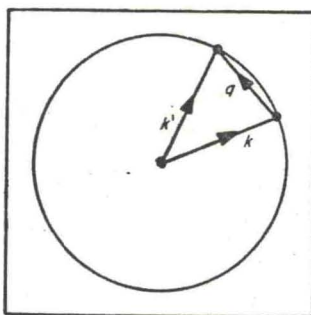


FIG. 16. Normal scattering process.

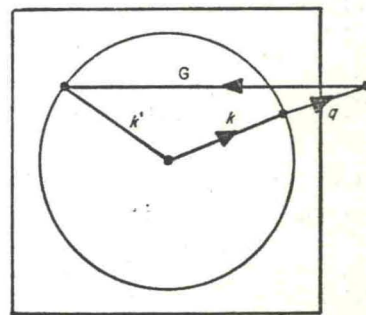


FIG. 17. Umklapp process.

The conservation of energy condition (equation 37) severely limits the possible scattering processes. This is because $\hbar\omega$ (which is of order kT for $T < \theta$ and of order $k\theta$ at higher temperatures) is so small compared to E_k that a phonon cannot significantly change the electron energy. Moreover since, at normal temperatures, kT itself is very small compared to E_F , there are unoccupied electron states only very close to the Fermi level; this in turn means that because of the Pauli principle only electrons close to the Fermi level (effectively on the Fermi surface) can be scattered and then only into other states (which must of course be unoccupied) that are themselves on the Fermi surface. This condition of scattering only from and to states on the Fermi surface is observed in all subsequent discussions and illustrations of scattering processes. (It applies, of course, equally to impurity scattering.)

In Figs. 16 and 17 a normal scattering process (or N-process) and a U-process are illustrated. In the example shown, the Fermi surface corresponds to a spherical surface and the Brillouin zone is shown as square for simplicity. The important point is that the Fermi surface

by the appropriate lattice

they provide a means by which information can be communicated. They also provide an immediate answer before provide an immediate answer. It is also important because G is small, U-processes make a significant contribution. This is particularly important

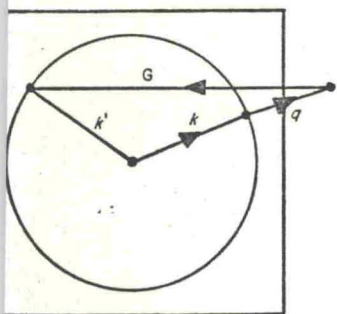


Fig. 17. Umklapp process.

Equation 37) severely limits the contribution because $\hbar\omega$ (which is of order kT at low temperatures) is so small that it does not significantly change the electron distribution. At low temperatures, kT itself is very small, and only very few electron states are excited. This is because of the Pauli exclusion principle (effectively on the order of kT) which prevents electrons from jumping into other states (which are empty) on the Fermi surface and to states on the Fermi surface. The following discussions and illustrations of the Umklapp process are equally applicable to impurity scatter-

ing. In the case of a U-process (or N-process) and as is shown, the Fermi surface does not touch the Brillouin zone boundary. It is at this point that the Fermi surface

does not touch the zone boundary and this corresponds to the case of the alkali metals at least at normal pressures. As we saw above, their Fermi surfaces are nearly spherical and do not touch the zone boundaries. (For the noble metals, however, the Fermi surfaces do touch the zone boundaries and the distinction between N- and U-processes is no longer useful.)

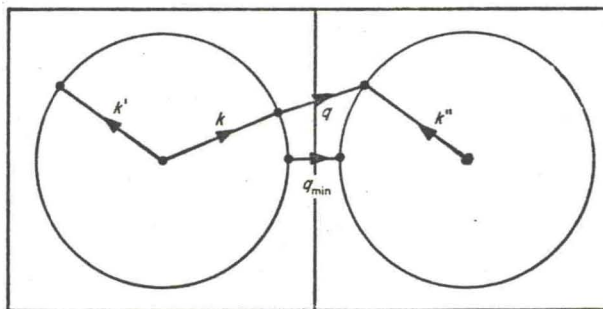


Fig. 18. A U-process in the repeated zone scheme showing minimum q vector for a U-process.

It is seen from Fig. 18 that when the Fermi surface does not touch the zone boundaries, there is a minimum value of q required to induce a U-process. Let us suppose that q_{\min} is this minimum value in a particular direction and that ω is the corresponding frequency of the phonon propagating in this direction. Then at low temperatures the number of such phonons excited is proportional to $e^{-\frac{\hbar\omega}{kT}}$. If c is the phonon velocity, this probability may be re-written in terms of q_{\min} as $e^{-\frac{\hbar cq_{\min}}{kT}}$. Clearly, therefore, under these circumstances, U-processes must die out at sufficiently low temperatures. On the other hand, their importance may persist down to quite low temperatures, if in some directions c is particularly small and q_{\min} not too large. Baily has shown that this is true in the alkali metals. These metals are very strongly anisotropic in their elastic properties and in certain directions there are low-lying transverse modes of vibration which can cause U-processes down to quite low temperatures. Moreover, because they almost reverse the electron momentum, these processes dominate the resistivity throughout the temperature region in which ρ_{ph} is still measurable (at the lowest temperatures ρ_{ph} is lost in the background of residual scattering).

The above expression for the probability of exciting a phonon which can induce an U-scattering process shows that the electrical resistivity at low temperatures is determined not only by the geometry of the Fermi surface (which determines the value of q_{\min} in any direction) but also by the elastic anisotropy of the crystal (which determines the value of c in any direction).

To understand the variation with pressure of electrical resistivity at low temperatures, therefore requires that we know both how the Fermi surface changes under pressure and how the elastic anisotropy changes under pressure. In addition to all this we must also know how the matrix elements for the electron phonon interaction change with pressure. Some of this information is, as we have seen, now available directly from experiment, but not all; a summary of the present situation is given in Table III.

B. TEMPERATURE AND PRESSURE DEPENDENCE OF RESISTIVITY AT VERY LOW TEMPERATURES

At sufficiently low temperatures where the phonon wavelengths are large compared to the interatomic distance, the continuum model of a solid gives a good description of the elastic vibrations in real solids. In this temperature region, the number of phonons varies as T^3 . On the other hand the electrical resistivity due to these phonons varies more rapidly; theoretically in the simplest case, it is expected to vary as T^5 . The reason for this is illustrated in Fig. 19 which shows that if an electron, travelling in the direction of the electric current, is scattered by a phonon of wave vector q through the angle Φ , as indicated, its momentum in the direction of the current is reduced by $(1 - \cos \Phi)$. If Φ is small, this approximates to $\frac{\Phi^2}{2}$. Now $\Phi \cong q/K_F$ and the magnitude of $q \propto T$.

To determine how the resistivity depends on temperature, we must take into account how the temperature alters both the number of scatterers (the phonons) and the effectiveness of each scattering process (i.e., the change in momentum induced). Consequently there is a factor of T^2 from this last effect in addition to the T^3 that arises from the variation of the number of phonons with temperature. If, therefore, we are at low enough temperatures so that the U-processes are frozen out, it can be shown that:

of exciting a phonon which at the electrical resistivity by the geometry of the of q_{\min} in any direction crystal (which determines the

ure of electrical resistivity at we know both how the how the elastic anisotropy his we must also know how on interaction change with e have seen, now available nmary of the present situa-

DEPENDENCE OF RESISTIVITY AT HIGH TEMPERATURES

the phonon wavelengths ance, the continuum model e elastic vibrations in real mber of phonons varies as ivity due to these phonons mplest case, it is expected ated in Fig. 19 which shows tion of the electric current, q through the angle Φ , as of the current is reduced by esto $\frac{\Phi^2}{2}$. Now $\Phi \approx q/K_F$

ds on temperature, we must alters both the number of ness of each scattering proed). Consequently there is a n to the T^3 that arises from h temperature. If, therefore, t the U-processes are frozen

$$\rho_{\text{ph}} \propto T^5/\theta^6 \tag{38}$$

where θ is the characteristic lattice temperature of the metal. If the volume of the metal is changed by pressure, θ alters and this provides one important mechanism for the change in resistivity with pressure at low temperatures.

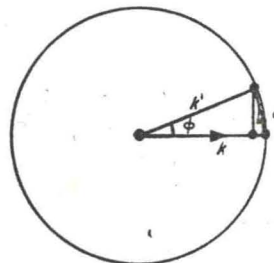


Fig. 19. Small angle scattering by phonons.

C. EFFECT OF TEMPERATURE AND PRESSURE ON ELECTRICAL RESISTIVITY AT HIGH TEMPERATURES

At high temperatures, i.e., $T \gtrsim \theta$, most of the phonons that are excited are of large q vector (typically about half the dimensions of the Brillouin zone) so that all collisions with phonons can produce a large change in the momentum of the conduction electrons. We may therefore expect that the electrical resistivity due to phonon scattering will depend directly on the number of phonons excited at a given temperature. Alternatively, looking at the problem in classical rather than quantum terms, we may expect the resistivity due to the lattice vibrations to be proportional to the mean square amplitude of these vibrations. In either case we write:

$$\rho_{\text{ph}} = K \frac{T}{M\theta^2} \tag{39}$$

where M is the mass of the ions that make up the lattice and K is a parameter that involves all the complex interactions between the conduction electrons and the ions.

If we compare equations (38) and (39) we see that at high temperatures ρ_{ph} depends inversely on θ^2 and at very low temperatures inversely on θ^6 . We also know that, in general, θ increases with in-

creased pressure.† Consequently we may expect a decrease of ρ_{ph} with pressure due to the change in θ to be very much bigger at low temperatures than at high (cf. Fig. 20, which illustrates this in the alkali metals).

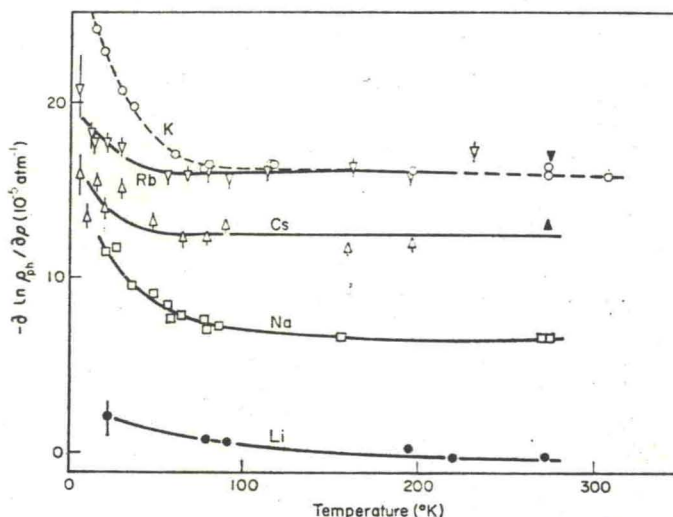


FIG. 20. Pressure coefficient of electrical resistivity in the alkali metals as a function of temperature. (From Dugdale and Phillips, 1965.)

More generally we may write:

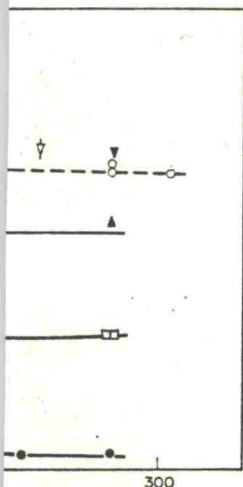
$$\rho_{ph} = \frac{K}{T} f(T/\theta) \quad (40)$$

where K has the same meaning as before and $f(T/\theta)$ is some universal function that varies as T^2/θ^2 at high temperatures and as T^6/θ^6 at low temperatures. Such a relationship is approximately true for several different metals and if we suppose that it is true for one metal under different pressures (with K and θ dependent on pressure) then we can relate the volume dependence of ρ_{ph} to its temperature dependence as follows (Dugdale, 1961; Dugdale and Guban, 1962):

$$\frac{\partial \ln \rho_{ph}}{\partial \ln V} = \frac{\partial \ln K}{\partial \ln V} + \frac{\partial \ln \theta}{\partial \ln V} \left(1 + \frac{\partial \ln \rho_{ph}}{\partial \ln T} \right) \quad (41)$$

† This may be seen crudely as follows. θ characterizes the vibrational frequencies ω of the lattice, and ω^2 in turn is proportional to the force constants, i.e., to the second derivatives of the atomic potential with respect to distance. The effect of pressure is to squeeze the potential well and hence to increase its curvature, i.e., essentially the force constants.

expect a decrease of ρ_{ph} with T much bigger at low temperatures. This is illustrated in the alkali metals.



(3) Resistivity in the alkali metals as a function of temperature (from Phillips, 1965.)

$$(40)$$

and $f(T/\theta)$ is some universal function of temperatures and as T^6/θ^6 at low temperatures (approximately true for several metals, it is true for one metal under independent on pressure) then we can describe its temperature dependence (from Guggenheim, 1962):

$$\frac{\partial \ln \rho_{ph}}{\partial \ln T} = \left(1 + \frac{\partial \ln \rho_{ph}}{\partial \ln T} \right) \quad (41)$$

characterizes the vibrational frequencies of the force constants, i.e., to increase with respect to distance. The effect of pressure is hence to increase its curvature,

In this expression we are treating K and θ and hence their volume derivatives as independent of temperature. Consequently if the electrical resistivity follows a reduced equation of state of the form shown in equation (40), we expect a linear relationship between the logarithmic volume derivative of ρ_{ph} and its logarithmic temperature derivative. This means that where the temperature dependence of ρ_{ph} changes rapidly with temperature the volume dependence will likewise change rapidly.

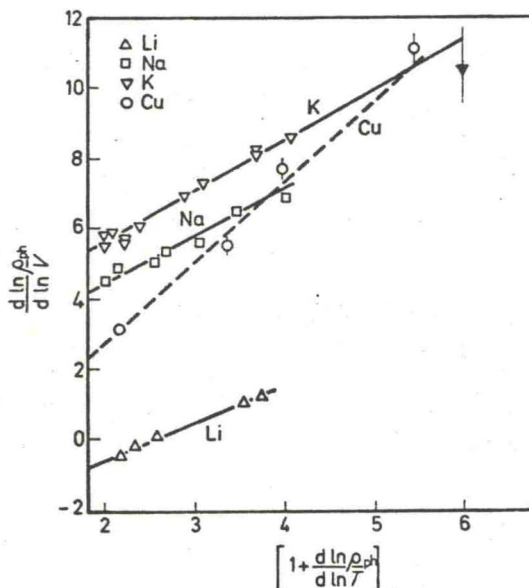


FIG. 21. Relationship between volume coefficient and temperature coefficient of resistivity. (From Dugdale, 1961.)

This relationship has been tested experimentally and the results are shown in Fig. 21 (Dugdale, 1961; Dugdale and Guggenheim, 1962). It is seen that a relationship of this kind does indeed hold. On the other hand we saw that the low-temperature behaviour of the electrical resistivity depended on both the shape of the Fermi surface and on the elastic anisotropy in a way that did not allow them to be separated in any simple fashion. This means that θ in equation (40) does not describe simply the lattice properties of the metal and so the reduced equation of state does not allow the lattice properties to be simply separated out from the electron properties as was originally hoped. The linear relationship in equation (41) is interesting and perhaps

useful, but not of any fundamental significance. It allows us to understand volume dependence at different temperatures in a phenomenological way but does not give us any deep insight into the processes.

D. CHANGE OF K WITH VOLUME

I have emphasized that at least at low temperatures the electrical resistivity depends sensitively on the relative proportions of N- and U-processes. This in turn depends on both the geometry of the Fermi surface and the anisotropy of the phonon-dispersion curves.

At high temperatures, however, where all scattering processes, whether N or U, involve large-angle scattering, it is probably more legitimate to separate out the dependence of the vibration amplitude (or the number of phonons) on volume from the other terms so that we can focus attention on the volume dependence of the electron-phonon interaction.

At high temperatures equation (39) applies. If we allow the pressure to vary at constant temperature we have from this equation:

$$\frac{\partial \ln \rho_{\text{ph}}}{\partial \ln V} = \frac{\partial \ln K}{\partial \ln V} - 2 \frac{\partial \ln \theta}{\partial \ln V} \quad (42)$$

In this expression we can estimate $\frac{\partial \ln \theta}{\partial \ln V}$ from the Grüneisen parameter; this in turn can be determined from purely equilibrium measurements on the metal since we have:

$$-\partial \ln \theta / \partial \ln V = \gamma = V \beta / \chi C_v \quad (43)$$

where β is the volume expansion coefficient, χ is the compressibility and C_v is the molar heat capacity at constant volume.

In this way we can estimate the change of θ with volume, and so determine the change of K with volume; cf. Table III. Table IV gives the results for the monovalent metals at 0° C. Our next problem is to understand the values of $\partial \ln K / \partial \ln V$ listed in the Table. Before considering the theoretical work that has been done on this, there are three further points about the variation of K with volume that must be brought out.

ance. It allows us to under-
 temperatures in a phenomeno-
 p insight into the processes.

VOLUME

temperatures the electrical
 ative proportions of N- and
 h the geometry of the Fermi
 n-dispersion curves.

scattering processes, wheth-
 g, it is probably more legit-
 the vibration amplitude (or
 the other terms so that we
 lence of the electron-phonon

lies. If we allow the pressure
 e from this equation:

$$2 \frac{\partial \ln \theta}{\partial \ln V} \quad (42)$$

from the Grüneisen param-
 purely equilibrium measure-

$$= V\beta/\chi C_v \quad (43)$$

ient, χ is the compressibility
 nstant volume.

age of θ with volume, and so
 e; cf. Table III. Table IV
 als at 0° C. Our next problem
 $\ln V$ listed in the Table. Be-
 t has been done on this, there
 ation of K with volume that

TABLE IV. Values of $\partial \ln K/\partial \ln V$

Metal	Experimental	Hasegawa (1964)	Theoretical (Dickey <i>et al.</i> , 1967)
Li	-2.3	-3.7	-1.1
Na	1.9	1.8	0.5
K	3.0	1.9	1.3
Rb	2.3	..	1.1
Cs	1.1†	..	-0.2

† There is considerable uncertainty in this value. According to Hasegawa (1964) some experimental values indicate it might be negative.

1. Relationship with Thermoelectric Power

If the electrical resistivity of a metal arises from effectively elastic scattering (e.g., impurity scattering or scattering by phonons at high temperatures), the thermoelectric power may be expressed as:

$$S = \frac{\pi^2 k^2 T}{3e} \left(\frac{\partial \ln \sigma(E)}{\partial E} \right)_{E=E_F} \quad (44)$$

(see, for example, Mott and Jones, 1936).

This relationship expresses the fact that under these circumstances and neglecting phonon drag the thermoelectric power should be linearly proportional to the absolute temperature; this is found experimentally, at least in the region of $T \sim \theta$. Moreover, the coefficient of proportionality should depend on the variation of the conductivity of the metal with the energy of the conduction electrons at the Fermi level. If we introduce the Fermi energy, E_F , measured from the bottom of the conduction band, we may rewrite equation (44) as follows:

$$S = \frac{\pi^2 k^2 T}{3e E_F} \frac{\partial \ln \sigma(e)}{\partial \ln E} \equiv \frac{\pi^2 k^2 T}{3e E_F} \xi \quad (44a)$$

In this way we can obtain from measured values of S , a value for the quantity ξ , which tells us how the electrical conductivity varies with energy.

It is then found that the quantity ξ evaluated in this way for the monovalent metals is closely related to the high-temperature value of the *volume* dependence of the electrical conductivity ($\partial \ln \sigma/\partial \ln V$). If we eliminate from this volume dependence the change in the ampli-

tude in the lattice vibrations (which has no counterpart in ξ) we are left with the quantity $\partial \ln K / \partial \ln V$. A comparison between this quantity and ξ shows that the two are approximately proportional to each other. This is illustrated in Fig. 22. This figure shows not only the

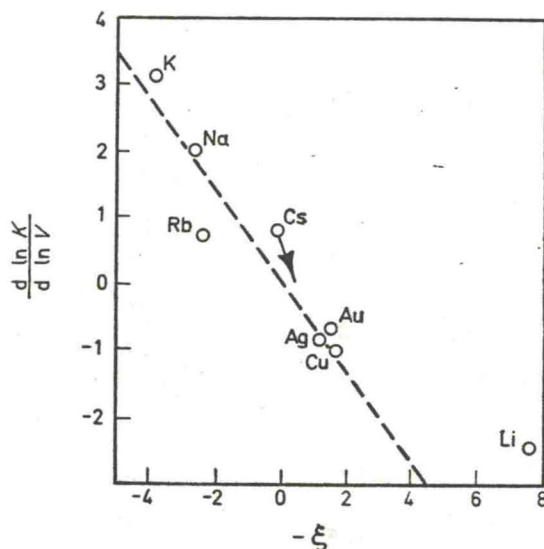


FIG. 22. Relationship between volume coefficient of K and thermoelectric power. Note that $-\xi$ is plotted. (From Dugdale and Mundy, 1961.)

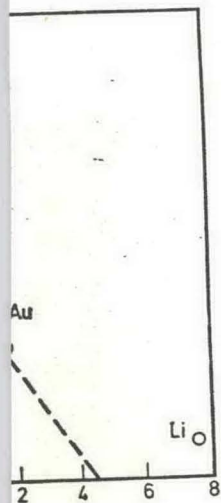
values of $\partial \ln K / \partial \ln V$ and ξ for the metals under *normal pressure*, but, for Cs, it shows values for the compressed metal. The approximate proportionality is still valid (Dugdale and Mundy, 1961).

A possible interpretation of this relationship is as follows. Assume that the electrical conductivity σ is a function only of the Fermi energy, E_F , the Debye temperature of the lattice, θ , and the temperature, T , i.e., we write $\sigma = \sigma(E_F, \theta, T)$; likewise the resistivity $\rho = 1/\sigma$ depends on the same variables. Then:

$$-\left(\frac{\partial \ln \rho}{\partial \ln V}\right)_T \equiv \left(\frac{\partial \ln \sigma}{\partial \ln V}\right)_T = \left(\frac{\partial \ln \sigma}{\partial \ln E_F}\right)_{\theta, T} \frac{d \ln E_F}{d \ln V} + \left(\frac{\partial \ln \sigma}{\partial \ln \theta}\right)_{E_F, T} \frac{d \ln \theta}{d \ln V} \quad (45)$$

This equation can be reduced on the basis of the following simplifying assumptions:

no counterpart in ξ) we are in comparison between this quantity and ξ is approximately proportional to each other. This figure shows not only the



coefficient of K and thermoelectric coefficient (see Mundy, 1961.)

metals under normal pressure, but, for a compressed metal. The approximate relationship is as follows. Assume K is a function only of the Fermi energy, θ , and the temperature, T ; likewise the resistivity $\rho = 1/\sigma$

$$\left(\frac{\partial \ln \sigma}{\partial \ln E_F} \right)_{\theta, T} \frac{d \ln E_F}{d \ln V} + \frac{d \ln \theta}{d \ln V} \quad (45)$$

on the basis of the following simpli-

$$\frac{d \ln \theta}{d \ln V} = -\gamma \quad (\text{the Grüneisen parameter})$$

$$\frac{\partial \ln \sigma}{\partial \ln \theta} = 2 \quad \text{at high temperatures (see equation 39 above)}$$

$$\frac{d \ln E_F}{d \ln V} = -\frac{2}{3} \quad \text{on the basis of the free-electron model or the effective mass approximation.}$$

Also:

$$\left(\frac{\partial \ln \sigma}{\partial \ln E_F} \right)_{\theta} = \xi \quad \text{as defined in equation (45)}$$

$$\therefore \left(\frac{\partial \ln \rho}{\partial \ln V} \right) - 2\gamma = \frac{2}{3} \xi$$

The left-hand side of this equation is just what we earlier denoted by $\partial \ln K / \partial \ln V$ so that the relationship between this quantity and ξ is established. The coefficient of proportionality on this simple treatment is just $\frac{2}{3}$, and this corresponds to the dashed line shown in Fig. 22.

The basis of this derivation is that σ depends on V only through E_F and θ , and that θ has no direct dependence on E_F . (It is a simple matter to generalize equation 45 for the situations where θ has an explicit E_F dependence.)

The experimental information thus suggests that these assumptions are approximately correct, i.e., the dependence of K on volume appears to arise largely from the change in E_F with V . This is an important fact which we will refer to again below.

2. The Behaviour of K at very high Pressures

So far we have considered only the initial slope of the resistivity-volume curves. On the other hand, considerable information is available about the pressure dependence of resistivity at room temperature up to quite high pressures. The experimental work of Bridgman (1949, 1952), for example, extends up to pressures of about 100,000 b at room temperature. Measurements to still higher pressures have been made by Stager and Drickamer (1963) not only at room temperature but also at low temperatures (see also Bundy, 1959; Balchou and Drickamer, 1961; Bundy and Strong 1962).

Figure 23 shows some of Bridgman's results in the form of relative resistivity versus relative volume for the alkali metals at room temperature. The notable feature of the curves in this Figure is that in Na, K and Rb the resistivity falls markedly with pressure and only begins to increase at very high pressures. By contrast the resistivity of Cs goes through a minimum at quite low pressures and then rises sharply: in Li the resistivity *increases* at all pressures in this range.

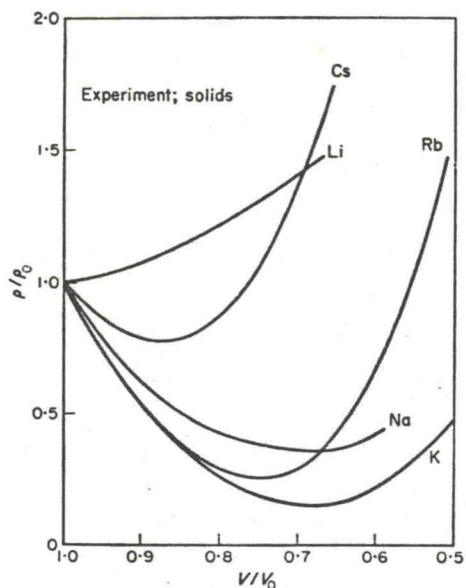
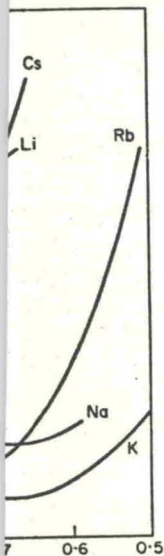


FIG. 23. Bridgman's results of the alkali metals at 0° C. The curves show relative resistance versus relative volume.

An important point in understanding these curves is as follows. No phase transitions occur in the pressure and temperature range under discussion so that we may be confident that the mean-square amplitude of the lattice vibrations decreases monotonically with increasing pressure for all the metals throughout this pressure range. The lattice vibrations by themselves, therefore, cannot account for the minima in these curves or for the positive slope of the Li curve. These effects must therefore be attributed to the change in K with volume. In order to emphasize this point the relative values of K versus relative volume for all the metals are shown in Fig. 24. (In order to obtain these curves, the change in θ with volume has been estimated from the compressibility of the metals.) It is clear that the main features of the ρ - V curve remain in the K - V curves.

results in the form of relative
alkali metals at room tem-
peratures in this Figure is that in-
creases steadily with pressure and only
slightly. By contrast the resistivity
decreases at low pressures and then rises
at all pressures in this range.



metals at 0° C. The curves show rela-

these curves is as follows. No
and temperature range under
study that the mean-square ampli-
tude increases monotonically with increasing
pressure in this pressure range. The lattice
model cannot account for the minima
of the Li curve. These effects
change in K with volume. In
Fig. 24. (In order to obtain
relative volume has been estimated from
the curves. It is clear that the main features
of these curves.

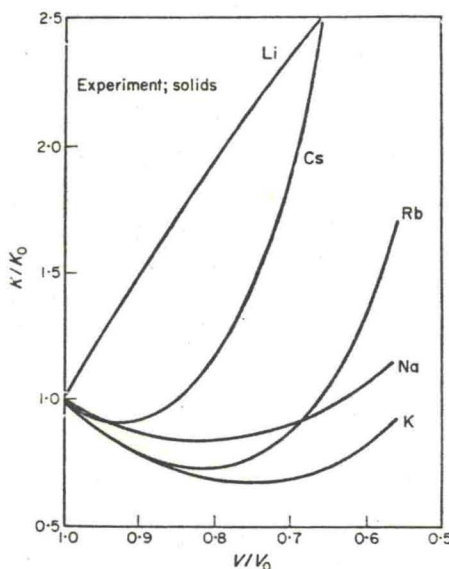


Fig. 24. K versus volume in the alkali metals deduced from the data in Fig. 23.

3. Comparison with Liquid Metals

The effect of pressure on the alkali metals in the liquid state has not been studied over such a wide range as for the solids. Bridgman has however made some measurements on the liquids. Of Cs he writes (Bridgman, 1949, p. 282): "Because of the location of the melting curve it was not possible to measure the resistance of the liquid metal at pressures high enough to reach the minimum [in the ρ - P curve], but simple extrapolation indicates that without much question the liquid will show the effect as well as the solid at temperatures above perhaps 140°, and there seems no reason to think that the mechanism responsible for the minimum has any essential connection with the lattice structure."

In Li, moreover, Bridgman finds that, as in the solid, the pressure coefficient of resistivity of the liquid is *positive* (in magnitude it is about 33% greater than that of the solid). In the other metals Bridgman finds negative pressure coefficients of resistivity of magnitude similar to those found in the corresponding solids.

To sum up what we know about the volume dependence of K : we know that: (1) at atmospheric pressure the sign of $\partial \ln K / \partial \ln V$ is different in different metals; (2) for the monovalent metals the sign of

$\partial \ln K / \partial \ln V$ correlates with the sign of the thermoelectric power. (There is also rough correlation between its magnitude and the quantity ξ derived from the temperature dependence of the thermo-power); (3) the variation of resistivity with volume over a wide range of volumes shows a rather diverse pattern of behaviour in the alkali metals; the behaviour of K is quite similar; (4) the variation of resistivity with volume in the liquid metals appears, as far as it is known, to be quite similar to that of the corresponding solids.

With these ideas in mind we will now look at some of the theoretical interpretations of how K depends on volume.

E. THEORETICAL WORK

As I have mentioned above, the conventional way of calculating electrical resistivity is to consider in detail the geometry of the scattering processes and this combined with a knowledge of the electron-phonon matrix elements and the phonon dispersion curves enables the resistivity to be calculated (cf. Bardeen, 1937; Ziman, 1954; Bailyn, 1960). To calculate how the resistivity varies with volume we must therefore know how all these features change under compression.

Bailyn (1960) made calculations of the effect of pressure on the resistivity of the alkali metals. In his model, the electron properties were derived from quantum-defect calculations although for simplicity the Fermi surfaces were treated as spherical both at normal pressure and under compression. Bailyn emphasized, however, that he did not expect the model to represent the behaviour of Li well. His results indicate a fall in electrical resistivity with pressure for all the alkali metals; they cannot therefore explain the rather diverse behaviour found by experiment.

Subsequently, it was generally supposed that the varied effects of pressure on resistivity could be explained in terms of the progressive distortion of the Fermi surface under pressure and that the different behaviour of the different metals was due to the different degrees of distortion (Cohen and Heine, 1958; Dugdale, 1961; Ham, 1962). The emphasis here was very much on the geometry of scattering, although of course the matrix elements themselves and the electron velocities would be altered. No detailed calculations were attempted and no quantitative estimates were made until the work of Hasegawa.

the thermoelectric power. magnitude and the quantity (ence of the thermo-power); over a wide range of volum- haviour in the alkali metals; the variation of resistivity s, as far as it is known, to be g solids.

ook at some of the theoretical lume.

WORK

ventional way of calculating il the geometry of the scatter- knowledge of the electron- on dispersion curves enables ardeen, 1937; Ziman, 1954; stivity varies with volume we res change under compression.

effect of pressure on the resis- , the electron properties were ns although for simplicity the l both at normal pressure and d, however, that he did not avioir of Li well. His results ith pressure for all the alkali the rather diverse behaviour

osed that the varied effects of ed in terms of the progressive pressure and that the different due to the different degrees of dgdale, 1961; Ham, 1962). The ometry of scattering, although ves and the electron velocities tions were attempted and no l the work of Hasegawa.

Hasegawa (1964) made calculations of the pressure dependence of the resistivity of Li, K and Na. In all three metals he assumed that the phonon anisotropy was essentially unchanged by pressure. Experiments have shown that this is true for Na and K, and approximately so for Li (see Table III). In Na and K, Hasegawa assumed that, the shape of the Fermi surfaces was also unchanged by pressure, i.e., that the surfaces remained effectively spherical. This means that in these two metals the geometry of the scattering processes is not altered by pressure, and therefore apart from the change in lattice vibrations the main effect of pressure is on the Fermi energy, the screening effects of the conduction electrons and on the matrix elements. In Li, on the other hand, Hasegawa had to take account of the distortion of the Fermi surface under pressure. In order to do this he used the results of Ham's calculations: these, as we saw above, almost certainly exaggerate the distortion of the Fermi surface both at normal pressure and under compression. Hasegawa's results are shown in Table IV and compared with the corresponding experimental data. It is seen that there is reasonable agreement between the two; on the other hand, because of the reliance on Ham's band structure calculations for Li, it is hard to judge how significant the agreement is in this case.

Dickey *et al.* (1967) used a different approach that has been remarkably successful in accounting for the main features of the pressure dependence of resistivity in the alkali metals. The model of a metal used by Dickey *et al.* is based on the idea of the neutral pseudo-atom (see for example, the exposition of this idea by Ziman, 1964).

The first problem to be tackled is that of a single ion of the metal under consideration immersed in a free-electron gas of the appropriate Fermi energy, i.e., the Fermi energy that corresponds to the volume of the metal occupied by the number of conduction electrons proper to that metal. Obviously, varying the volume of the metal will vary the Fermi energy. A calculation is now made, in terms of phase shifts, of the scattering of electrons at the Fermi energy by the potential due to this ion. The potential of the ion is a combination of:

- (1) The electron-ion potential; this is derived for the free ion by means of a Hartree-Fock-Slater calculation (and is taken over from existing calculations).
- (2) A screening potential chosen to satisfy the Friedel sum rule. This rule essentially ensures that the screening charge around any ion is just sufficient to provide electrical neutrality.

The screening in the Dickey-Meyer-Young model is chosen to have the simplest form consistent with eliminating the long-range coulomb field of the ion. It is therefore chosen to be of the form of the coulomb potential of a single charge outside a radius r_0 and to be constant inside this radius. r_0 is then chosen to satisfy the Friedel sum rule. It is thus equivalent to spherical shell of charge of suitable radius.

In this way a set of phase-shifts, η_l is obtained for each metal at several different volumes. A change in volume alters the Fermi level, as mentioned above, and also the screening radius.

So far the calculation is for a single individual screened ion. In order to calculate the properties of the metal (either solid or liquid), a suitable array of these ions is assembled; the resistivity is then calculated on the basis of a structure factor appropriate to this array. The relevant expression for the electrical resistivity is then as follows (based on a Debye model to deduce the structure factor):

$$\rho = \frac{2^{2/3} (\hbar k_F)^3 \sigma_R k_B T}{e^2 M (k_B \theta)^2} \quad (46)$$

where:

$$\sigma_R = (4\pi/k_F^2) \sum_l l \sin^2(\eta_{l-1} - \eta_l) \quad (47)$$

Here θ is the Debye temperature, k_B Boltzmann's constant, e the electronic charge and k_F the Fermi radius. It is therefore clear that the expression (46) has the same form as that already discussed and that the parameter K introduced earlier can be evaluated as:

$$K = \frac{2^{2/3} (\hbar k_F)^3 \sigma_R}{k_B e^2} \quad (48)$$

All details of the phonon spectrum, U- and N-processes, have been left out. The feature that has been carefully retained, by means of the phase-shift calculation, is the detail of the scattering potential. Now let us look at the results.

Figure 25 shows how the phase shifts vary with volume for Li, K and Cs. In Li, the p phase shift is dominant throughout. In K, the s , p and d phase shifts are all comparable, although the d phase shift tends to dominate at the highest compressions. In Cs, the d phase shift is important, though not dominant, from the outset and its importance increases with compression.

ung model is chosen to have
ting the long-range coulomb
e of the form of the coulomb
s r_0 and to be constant inside
e Friedel sum rule. It is thus
suitable radius.

obtained for each metal at
olume alters the Fermi level,
ing radius.

individual screened ion. In
metal (either solid or liquid),
d; the resistivity is then cal-
or appropriate to this array.

resistivity is then as follows
structure factor):

$$\frac{k_B T}{\dots} \quad (46)$$

$$\eta_{i-1} - \eta_i \quad (47)$$

Boltzmann's constant, e the
. It is therefore clear that the
t already discussed and that
be evaluated as:

$$\sigma_R \quad (48)$$

- and N-processes, have been
lly retained, by means of the
he scattering potential. Now

vary with volume for Li, K
inant throughout. In K, the
le, although the d phase shift
pressions. In Cs, the d phase
nt, from the outset and its

The physical origin of these effects can perhaps be understood as follows. In the free ion the possible electron states are bound levels, of which some are occupied. The occupied levels are the X-ray levels; above these are unoccupied levels, and transitions of an electron from one of these to another gives rise to the characteristic atomic spectrum of the element.

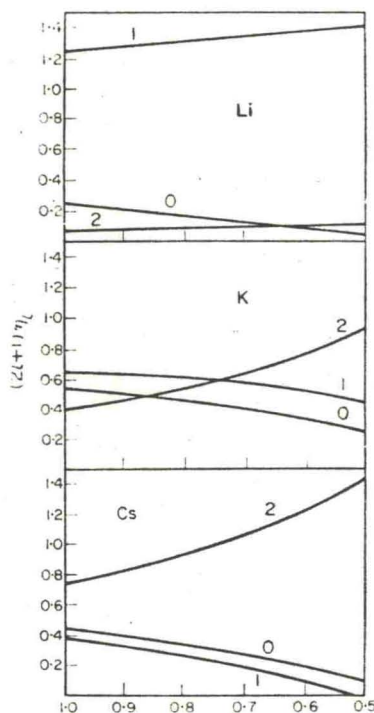


FIG. 25. Phase shifts in Li, K and Cs and the functions of relative volume. (From Dickey *et al.*, 1967.)

In the metal the X-ray levels remain filled. On the other hand, the outermost electron (in a monovalent metal there is just one of these per atom) forms part of the gas of conduction electron which, for simplicity, is here treated as a Fermi-Dirac gas of free particles confined to the volume of the metal. These particles in the Fermi gas screen the ion and, because of this, all the electron levels of the free ion are raised in energy. This in turn causes the unoccupied levels to lie in the continuum of levels available to the electron gas (cf. Fig. 26).

ly raised in energy. Those
eract with these states and
onance is so broad as to be
ered as the principle origin
of the free ion are broaden-
els are near the Fermi level
h is reflected in an enhance-

The main effect of pressure is to alter the Fermi level. Pressure also alters the screening and hence the height of all the energy levels of the ions, but this second effect is slight. In Cs, the effect of compression is to raise the Fermi level towards the *d* resonance corresponding to the empty *d* bound state of the free ion. This accounts for the gradual enhancement of the *d* phase shift on compression (see Fig. 25). Likewise in Li, the *p* resonance has a dominant effect on the phase shifts. Similar though less conspicuous effects occur in the other metals.

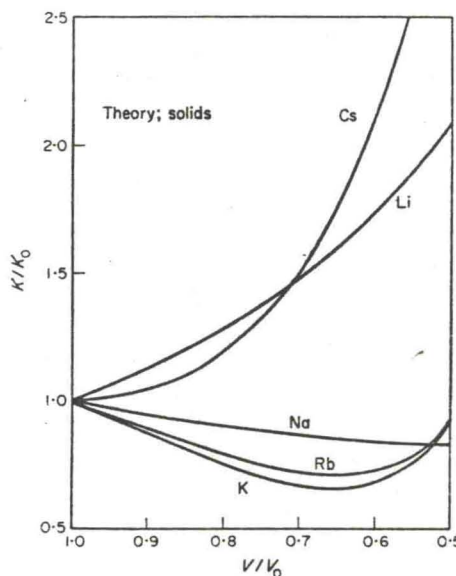
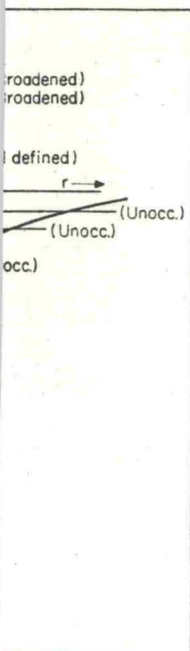


FIG. 27. Calculated K versus volume in the alkali metals (from Dickey *et al.*, 1967) to be compared with Fig. 24.

As Dickey *et al.* point out, their discussion is in some ways similar to the point of view put forward by Fermi and verified quantitatively by Sternheimer (1950) to account for the phase transition found in Cs by Bridgman at about 45 kb pressure.

We return now to the calculation of electrical resistivity. It is clear from equation (47) for the resistivity scattering cross-section, that if one phase shift is large compared to the others, this tends to produce a high resistivity. The detailed calculations of the change of resistivity with volume for the whole alkali metal series confirm this and show how the rise in resistivity under compression in Li at all volumes and in Cs after slight compression are reproduced by theory (Fig. 27). In

ion in a metal. The free-ion levels
corresponding levels in the metal
the unexcited free atom. (From

d rather crudely as follows.
energy would be *bound* in the
may be thought of as bound
the continuum. The potential
"memory" of the free-ion poten-

fact a comparison between Figs 24 and 27 shows that the theory reproduces qualitatively all the features found experimentally (see also Table IV).

The *absolute* magnitudes of the resistivities are *not* given accurately by the theory, presumably because of the crude approximations in the treatment of the phonons. The fact that the *relative* changes with volume are well reproduced shows that these diverse effects of pressure arise from the *details of the scattering potential* rather than from details of the phonon spectrum or of the Fermi surface. These are conclusions that we saw were suggested by other experimental features of the transport properties of the alkali metals and are fully confirmed by the calculations of Dickey *et al.*

From the model itself it is possible also to calculate the thermoelectric power and its variations with pressure. The thermoelectric power is rather a subtle property, since its calculation requires a knowledge of the energy dependence of the electron scattering. Nevertheless, the theory is reasonably successful in accounting for the magnitudes of the thermoelectric power (at high temperatures, where phonon scattering is dominant) and also for some important features of their pressure dependence (see Table V). In a subsequent article in this series Professor N. H. March discusses pressure effects in metals from a theoretical point of view (Vol. 3).

TABLE V. ξ and its volume derivative, derived from the thermoelectric power of the solid alkali metals at 0° C

Metal	ξ		$\partial \ln \xi / \partial \ln V$	
	experiment	theory	experiment	theory
Li	-6.7	-0.7	-0.24	-0.5
Na	2.7	2.4	1.4	0.61
K	3.8	3.2	-1.0	0.35
Rb	2.3	3.3	-0.3	0.27
Cs	0.2	0.6	~50	19

F. IMPURITY SCATTERING

The effect of pressure on the resistivity due to impurities, ρ_0 , has been studied quite extensively in the noble metals by Linde (for a summary, see Gerritsen, 1956). Further work has been reported since then (Dugdale, 1965b). The important feature of the measurements by Dugdale and Phillips (reported in Dugdale, 1965b)

LOW TEMPERATURES

7 shows that the theory re-
and experimentally (see also

ies are *not* given accurately
rude approximations in the
the *relative* changes with
se diverse effects of pressure
total rather than from details
rface. These are conclusions
perimental features of the
d are fully confirmed by the

to calculate the thermoelec-
e. The thermoelectric power
lation requires a knowledge
cattering. Nevertheless, the
nting for the magnitudes
mperatures, where phonon
me important features of
In a subsequent article in
es pressure effects in metals

ative, derived from
alkali metals at 0° C

$\partial \ln \xi / \partial \ln V$	
experiment	theory
-0.24	-0.5
1.4	0.61
-1.0	0.35
-0.3	0.27
50	19

ING

r due to impurities, ρ_0 , has
ble metals by Linde (for a
ork has been reported since
feature of the measure-
ted in Dugdale, 1965b)

is that they were made at 4.2° K (by the helium gas technique). This meant that it was possible to measure the effect of pressure on the residual resistivity of the noble metals containing *other noble metals* as impurity. Since these impurities cause relatively little scattering, this can hardly be done at room temperature when the phonon scattering would dominate (at least in dilute alloys).

What all these results emphasize is the variety of values (of both signs) that are found for $\partial \ln \rho_0 / \partial \ln V$. This presumably again arises from the details of the potentials of the scatterers; here we are concerned with the difference in potential between the impurity and the host lattice. To make realistic comparison between theory and experiment demands careful calculations similar to (but perhaps more difficult than) those of Dickey *et al.* (1967) on the alkali metals already referred to. These authors have in fact made calculations of the resistivities due to noble metal impurities in the noble metals themselves, but they conclude that their model is not very satisfactory for these systems. This is presumably partly because of the distorted Fermi surfaces in the noble metals but mainly because of the low lying *d* levels which overlap to form a band and so alter substantially the electronic structure of these metals.

G. PHONON AND IMPURITY SCATTERING BOTH PRESENT

The effect of pressure on electrical resistivity due to phonons at low temperatures is almost invariably deduced from measurements on specimens whose resistivity is dominated by impurity scattering (cf. Fig. 28). This can give rise to error in the following way.

Recent work (Dugdale and Basinski, 1967) has focused attention on departures from Matthiessen's rule when two (or more) scattering mechanisms are present in the same metal with different anisotropies of relaxation times $\tau(k)$. The departure from Matthiessen's rule is measured by a quantity Δ defined as follows:

$$\Delta = \rho_{\text{meas}} - \rho_{\text{ph}} - \rho_0 \tag{49}$$

ρ_{meas} is the measured resistivity of the specimen at some temperature *T*, ρ_{ph} is the resistivity of an ideally pure sample at the same temperature and ρ_0 the resistivity measured at very low temperatures where ρ has ceased to depend on temperature.

Normally one assumes that Matthiessen's rule holds and that $\Delta = 0$. Thus:

$$\rho = \rho_{\text{ph}} + \rho_0 \quad (50)$$

and so:

$$\frac{\partial \ln \rho}{\partial \ln V} = \frac{\rho_{\text{ph}}}{\rho} \frac{\partial \ln \rho_{\text{ph}}}{\partial \ln V} + \frac{\rho_0}{\rho} \frac{\partial \ln \rho_0}{\partial \ln V} \quad (51)$$

So if one measures $\frac{\partial \ln \rho}{\partial \ln V}$ at the temperature of interest and $\frac{\partial \ln \rho_0}{\partial \ln V}$ at some very low temperature, $\frac{\partial \ln \rho_{\text{ph}}}{\partial \ln V}$ can be deduced from these values and those of ρ and ρ_0 .

Now suppose that instead of equation (50) we use the correct equation (49):

$$\rho_{\text{meas}} = \rho_{\text{ph}} + \rho_0 + \Delta \quad (52)$$

Then we get:

$$\frac{\partial \ln \rho}{\partial \ln V} = \frac{\rho_{\text{ph}}}{\rho} \frac{\partial \ln \rho_{\text{ph}}}{\partial \ln V} + \frac{\rho_0}{\rho} \frac{\partial \ln \rho_0}{\partial \ln V} + \frac{\Delta}{\rho} \frac{\partial \ln \Delta}{\partial \ln V} \quad (53)$$

In dilute noble-metal alloys (Dugdale and Basinski, 1967), it is found that with Au in Ag or Cu, Δ at the lowest temperatures is similar in magnitude or greater than ρ_{ph} . This would mean that if one deduced $\partial \ln \rho_{\text{ph}} / \partial \ln V$ from low-temperature measurements on such alloys, assuming Matthiessen's rule, the result would be a factor or two or more too large. Similar (though probably slightly smaller) errors would be found with other impurities.

An experimental example of how departures from Matthiessen's rule affect the deduced values of $\partial \ln \rho_{\text{ph}} / \partial \ln V$ is seen in the measurements of Dugdale and Phillips (1965) on two samples of Rb of very different purity (see Table 5 of their publication.) The less pure specimen shows a much bigger apparent volume coefficient of phonon induced resistivity than the purer one.

V. SOME CONCLUSIONS

In order to understand the effect of pressure on electrical resistivity at low temperatures ($T \lesssim \theta/3$) we have to know how the properties of the Fermi surface, the phonon velocities and electron-phonon

's rule holds and that $\Delta = 0$.

$$(50)$$

$$\frac{\rho_0}{\rho} \frac{\partial \ln \rho_0}{\partial \ln V} \quad (51)$$

ature of interest and $\frac{\partial \ln \rho_0}{\partial \ln V}$

can be deduced from these

50) we use the correct equa-

$$+ \Delta \quad (52)$$

$$\frac{\ln \rho_0}{\ln V} + \frac{\Delta}{\rho} \frac{\partial \ln \Delta}{\partial \ln V} \quad (53)$$

d Basinski, 1967), it is found
st temperatures is similar in
d mean that if one deduced
asurements on such alloys,
ould be a factor or two or
slightly smaller) errors would

partures from Matthiessen's
 $\partial \ln V$ is seen in the measure-
two samples of Rb of very
ation.) The less pure specimen
efficient of phonon induced

USIONS

ssure on electrical resistivity
to know how the properties
ocities and electron-phonon

matrix elements vary with pressure. At higher temperatures, this information is still needed, but recent work by Dickey *et al.* has shown that the main features of the volume dependence of resistivity, at least in the alkali metals, depend on the electron-ion potential. The full detail of this potential must be retained if the model is to reproduce the more important features of the experimental results. To get detail-

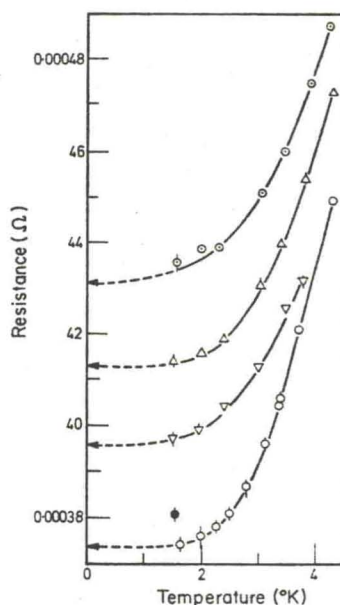


FIG. 28. Resistance versus temperature in Rb at various pressures at low temperatures. (From Dugdale and Phillips, 1965.)

ed numerical agreement will presumably require *both* this careful treatment of the potential *and* a more accurate treatment of the scattering geometry. For the present, however, the important thing is that the potential plays a vital role in these calculations.

This lesson would appear also to apply to the noble metals. Indeed many of the perplexing features of the transport properties of the monovalent metals (e.g., the anomalous sign of the thermo-power at high temperatures in Li, Cu, Ag, Au) may be resolved by paying more attention than hitherto to the electron-ion potential itself.

The work discussed in this article has been determined largely by my own interests. Nevertheless, here as elsewhere, there is now a clear and welcome trend in high-pressure physics: the theory is begin-

ning to be understood. The subject has for too long been characterized by an abundance of data and a dearth of understanding. The position is now changing fast.

ACKNOWLEDGMENTS

I am grateful to Dr P. J. Melz, Dr J. E. Schirber, Dr I. M. Templeton and Dr W. H. Young for access to their results before publication. I would also like to thank Dr M. Bailyn and Dr A. Myers for reading the manuscript and commenting on it.

REFERENCES

- Anderson, J. R. and Gold, A. V. (1965). *Phys. Rev.* **139**, A 1459.
 Anderson, J. R., O'Sullivan, W. J. and Schirber, J. R. (1967). *Phys. Rev.* **153**, 721.
 Ashcroft, N. W. (1963). *Phil. Mag.* **8**, 2055.
 Bailyn, M. (1960). *Phys. Rev.* **120**, 381.
 Balain, K. S., Grenier, C. G. and Reynolds, J. M. (1960). *Phys. Rev.* **119**, 935.
 Balchan, A. B. and Drickamer, H. G. (1961). *Rev. scient. Instrum.* **32**, 308.
 Bardeen, J. (1937). *Phys. Rev.* **52**, 608.
 Berlincourt, T. G. and Steele, M. C. (1954). *Phys. Rev.* **95**, 1421.
 Brandt, N. B. and Ginzburg, N. I. (1962). *Soviet Phys. Solid St.* **3**, 2510.
 Bridgman, P. W. (1949). "The Physics of High Pressure". Bell, London.
 Bridgman, P. W. (1952). *Proc. Am. Acad. Arts Sci.* **81**, 167.
 Bundy, F. P. (1959). *Phys. Rev.* **115**, 274.
 Bundy, F. P. and Strong, H. M. (1962). *Solid St. Phys.* **13**, 81.
 Burdick, G. A. (1963). *Phys. Rev.* **129**, 138.
 Caroline, D. and Schirber, J. E. (1963). *Phil. Mag.* **8**, 71.
 Chambers, R. G. (1962). "Fermi Surface", ed. by W. A. Harrison and M. B. Wiley, Webb. New York.
 Cohen, M. H. and Heine, V. (1958). *Adv. Phys.* **7**, 395.
 Davis, H. L., Faulkner, J. S. and Joy, H. W. (1968). *Phys. Rev.*, **167**, 601.
 Deutsch, T., Paul, W. and Brooks, H. (1961). *Phys. Rev.* **124**, 753.
 Dickey, J. M., Meyer, A. and Young, W. H. (1967). *Proc. Phys. Soc.* **92**, 460.
 Dmitrenko, I. M., Verkin, B. I. and Lazarev, B. G. (1959). *Soviet Phys. JEPT* **8**, 229.
 Drickamer, H. G. (1963). *Solid St. Phys.* **17**, 1.
 Dugdale, J. S. (1958). *Nuovo Cim., Suppl.* **9**, 27.
 Dugdale, J. S. (1961). *Science*, N. Y. **134**, 177.
 Dugdale, J. S. (1965a). In "Physics of Solids at High Pressures", ed. by C. T. Tomizuka and R. M. Emrick, p. 16. Academic Press, New York. In Table 2 of this paper, the sign of $\partial \ln \rho / \partial \ln V$ for Cu in Ag should be negative.
 Dugdale, J. S. (1965b). "Physics at High Pressures and the Condensed Phase", ed. by A. Van Itterbeek, p. 382. North-Holland, Amsterdam.
 Dugdale, J. S. and Basinski, Z. S. (1967). *Phys. Rev.* **157**, 552.
 Dugdale, J. S. and Guban, G. (1962). *Proc. Roy. Soc. A* **270**, 186.
 Dugdale, J. S. and Hulbert, J. A. (1957). *Can. J. Phys.* **35**, 720.
 Dugdale, J. S. and Mundy, J. N. (1961). *Phil. Mag.* **6**, 1463.
 Dugdale, J. S. and Phillips, D. (1965). *Proc. Roy. Soc. A* **287**, 381.
 Fawcett, E. (1964). *Adv. Phys.* **13**, 139.

too long been characterized understanding. The position

ENTS

J. Schirber, Dr I. M. Temple-
their results before publica-
Bailyn and Dr A. Myers for
on it.

Rev. **139**, A 1459.
er, J. R. (1967). *Phys. Rev.* **153**,

. M. (1960). *Phys. Rev.* **119**, 935.
Rev. scient. Instrum. **32**, 308.

Phys. Rev. **95**, 1421.
Soviet Phys. Solid St. **3**, 2510.
gh Pressure". Bell, London.
Sci. **81**, 167.

St. Phys. **13**, 81.

. *Mag.* **8**, 71.
i. by W. A. Harrison and M. B.

Phys. **7**, 395.
W. (1968). *Phys. Rev.*, **167**, 601.
Phys. Rev. **124**, 753.
1967). *Proc. Phys. Soc.* **92**, 460.
B. G. (1959). *Soviet Phys. JETP*

27.

at High Pressures", ed. by C. T.
emic Press, New York. In Table 2
r Cu in Ag should be negative.
ssures and the Condensed Phase",
olland, Amsterdam.
Phys. Rev. **157**, 552.
Roy. Soc. A **270**, 186.
t. *J. Phys.* **35**, 720.
t. *Mag.* **6**, 1463.
Roy. Soc. A **287**, 381.

- Gaidukov, Yu. P. and Itskevich, E. S. (1963). *Zh. eksp. teor. Fiz.* **45**, 71 (*Soviet Phys. JETP* 1964, **13**, 51).
Gerhardt, U. (1968). *Phys. Rev.*, **172**, 651.
Gerritsen, A. N. (1956). "Encyclopedia of Physics", Vol. XIX, p. 137. Pergamon Press, London.
Goree, W. S. and Scott, T. A. (1966). *J. Phys. Chem. Solids* **27**, 835.
Ham, F. S. (1962). *Phys. Rev.* **128**, 82, 2524.
Harrison, W. A. (1959). *Phys. Rev.* **116**, 555.
Harrison, W. A. (1960). *Phys. Rev.* **113**, 1182.
Harrison, W. A. (1965). In "Physics of Solids at High Pressures", ed. by C. T. Tomizuka and R. M. Emrik, p. 13. Academic Press, New York.
Harrison, W. A. (1966). "Pseudo-potentials in the Theory of Metals". Benjamin, New York.
Hasegawa, A. (1964). *J. Phys. Soc. Japan* **19**, 504.
Hatton, J. (1955). *Phys. Rev.* **100**, 681.
Higgins, R. J. and Marcus, J. A. (1966). *Phys. Rev.* **141**, 553.
Hinrichs, C. H. and Swenson, C. A. (1961). *Phys. Rev.* **123**, 1106.
Itskevich, E. S. (1964). *Cryogenics*, 365.
Itskevich, E. S., Voronovskii, A. N. and Sukhoparov, V. A. (1965). *Soviet Phys. JETP Letters* **2**, 42.
Jan, J.—P. (1957). *Solid St. Phys.* **5**, 3.
Jan, J.—P. (1966). *Physics Can.* **22**, 6.
Kan, L. and Lazarew, B. (1958). *Soviet Phys. JETP* **7**, 180.
Landwehr, G. (1965). "Physics at High Pressures and the Condensed Phase", ed. by A. Van Itterbeek, p. 556. North-Holland, Amsterdam.
Lawson, A. W. (1956). *Progr. Metal Phys.* **6**, 1.
Lazarew, B. G. and Kan, L. S. (1944). *Zh. eksp. teor. Fiz.* **14**, 439.
Levy, M. and Olsen, J. L. (1965). "Physics at High Pressures and the Condensed Phase", ed. by A. Van Itterbeek, p. 525. North-Holland, Amsterdam.
Lifshitz, I. M. (1960). *Soviet Phys. JETP* **11**, 1130.
Lifshitz, I. M. and Peshanskii, V. G. (1958). *Zh. eksp. Fiz.* **35**, 1251 (English trans. *Soviet Phys. JETP* 1959, **3**, 875.).
Melz, P. J. (1966a). Ph. D. Thesis, University of Illinois.
Melz, P. J. (1966b). *Phys. Rev.* **152**, 540.
Mott, N. F. and Jones, H. (1936). "Theory of the Properties of Metals and Alloys", Clarendon Press, Oxford.
Okumura, K. and Templeton, I. M. (1965). *Proc. Roy. Soc. A* **287**, 89.
O'Sullivan, W. J. and Schirber, J. E. (1966). *Phys. Rev.* **151**, 484.
O'Sullivan, W. J., and Schirber, J. E. (1968). *Phys. Rev.*, **170**, 667.
Paul, W. (1963). "High Pressure Physics and Chemistry", ed. by R. S. Bradley. Academic Press, London.
Pippard, A. B. (1960). *Rept. Progr. Phys.* **XXIII**, 176.
Roaf, D. J. (1962). *Phil. Trans. Roy. Soc.* **255**, 135.
Schirber, J. E. (1965). *Phys. Rev.* **140**, 2065.
Schirber, J. E. and Swenson, C. A. (1961). *Phys. Rev.* **123**, 1115.
Schirber, J. E. and Swenson, C. A. (1962). *Phys. Rev.* **127**, 72.
Segall, B. (1962). *Phys. Rev.* **125**, 109.
Shoenberg, D. (1957). "Progress in Low Temperature Physics", ed. by C. J. Gorter, Vol. II, p. 226. North-Holland, Amsterdam.
Shoenberg, D. (1962). *Phil. Trans. Roy. Soc.* **255**, 85.
Shoenberg, D. and Stiles, P. J. (1964). *Proc. Roy. Soc. A* **281**, 62.
Shoenberg, D. and Watts, B. R. (1965). *IX th Int. Cong. low Temp. Phys.* ed. by J. G. Daunt, D. O. Edwards, F. S. Milford and M. Yaqub. Plenum Press, New York.
Shubnikov, L. and de Haas, W. J. (1930). *Communs phys. Lab. Univ. Leiden* 207 (d).
Sizoo, G. J. and Onnes, H. K. (1925). *Communs phys. Lab. Univ. Leiden* 180 (b).
Sizoo, G. J., de Haas, W. J. and Onnes, H. K. (1925). *Communs phys. Lab. Univ. Leiden* 180 (d).

- Stager, R. A. and Drickamer, H. G. (1963). *Phys. Rev.* **132**, 124.
- Sternheimer, R. (1950). *Phys. Rev.* **78**, 235 (see also the interesting recent work of Jayaraman, A., Newton, R. C. and McDonough, J. M. (1967). *Phys. Rev.* **159**, 527).
- Stewart, A. T., Donaghy, J. J., Kusmiss, J. H. and Rockmore, D. M. (1964). *Bull. Am. Phys. Soc.* **9**, 238.
- Stewart, J. W. (1965). "Physics at High Pressures and the Condensed Phase", ed. by A. Van Itterbeek, p. 189. North Holland, Amsterdam.
- Swenson, C. A. (1964). In "A. I. M. E. Symposium, Dallas, Texas", ed. by K. A. Gschneidner Jr., Gordon and Breach, New York.
- Templeton, I. M. (1966). *Proc. Roy. Soc. A* **292**, 413.
- Vasvári, B. and Heine, V. (1967). *Phil. Mag.* **14**, 731.
- Vasvári, B., Animabe, A. O. E. and Heine, V. (1967). *Phys. Rev.* **154**, 535.
- Verkin, B. I. and Dmitrenko, I. M. (1959) *Soviet Phys.* **4**, 118.
- Ziman, J. M. (1954). *Proc. Roy. Soc. A* **226**, 436.
- Ziman, J. M. (1964). *Adv. Phys.* **13**, 89.